

EXTRACTION OF ELECTROMAGNETIC PROPERTIES OF METAMATERIALS WITH  
BRANCH COMPENSATION FROM PHASE TRACKING

A Thesis  
Submitted to the Graduate Faculty  
of the  
North Dakota State University  
of Agriculture and Applied Science

By  
Jacob Christian Lewis

In Partial Fulfillment of the Requirements  
for the Degree of  
MASTER OF SCIENCE

Major Department:  
Electrical and Computer Engineering

July 2020

Fargo, North Dakota

# NORTH DAKOTA STATE UNIVERSITY

Graduate School

---

## Title

EXTRACTION OF ELECTROMAGNETIC PROPERTIES OF  
METAMATERIALS WITH BRANCH COMPENSATION FROM PHASE  
TRACKING

---

## By

Jacob Christian Lewis

---

The supervisory committee certifies that this thesis complies with North Dakota State University's regulations and meets the accepted standards for the degree of

MASTER OF SCIENCE

## SUPERVISORY COMMITTEE:

Dr. Benjamin D. Braaten

---

Chair

Dr. Ivan Lima

---

Dr. Alan Denton

---

Approved:

July 15, 2020

---

Date

Dr. Benjamin D. Braaten

---

Department Chair

# ABSTRACT

In the field of electromagnetism, there are materials known as metamaterials which exhibit unique properties that can be exploited. Permittivity, defined as capacitance per meter, of a metamaterial can vary over frequency, time, or even be negative. This can be useful for tuning antennas, changing their operating frequency or direction of propagation, or even designing cloaking systems. However, the theory behind metamaterials needs to be studied further. One of the biggest issues to address is in determining the constitutive parameters of metamaterials which may be varying. Previous research has shown the issue of branches, or mathematical discontinuities, occurring in the derivation of permittivity from the scattering parameters of a metamaterial. This thesis provides further understanding to the theory behind these branches and presents a new method to compensate for them. This new method, called the phase tracking method, may be considered a modern adaptation of the Nicolson-Ross-Weir method.

## ACKNOWLEDGEMENTS

This thesis was heavily influenced by a question proposed by Dr. Benjamin Braaten in 2018, and was based on his work with Jerika Cleveland, Dipankar Mitra, Dr. Jeffrey Alan, and Dr. Monica Alan. The question was originally based on a book example from Constantine A. Balanis' book, *Advanced Engineering Electromagnetics*. This team has aided me in this research, for which I am quite grateful!

## DEDICATION

To the parents who support me, wife who loves me, and Jesus who gives me life beyond my imagination. Thank you.

# TABLE OF CONTENTS

ABSTRACT . . . . .	iii
ACKNOWLEDGEMENTS . . . . .	iv
DEDICATION . . . . .	v
LIST OF TABLES . . . . .	viii
LIST OF FIGURES . . . . .	ix
LIST OF ABBREVIATIONS . . . . .	xi
LIST OF SYMBOLS . . . . .	xii
1. INTRODUCTION . . . . .	1
1.1. Context . . . . .	1
1.2. Previous Work . . . . .	1
1.3. Setup . . . . .	2
1.4. Assumptions . . . . .	3
2. DERIVING EQUATIONS FROM BOUNDARY CONDITIONS . . . . .	5
2.1. Signals . . . . .	5
2.2. Derivation of System Reflection . . . . .	7
2.3. Derivation of System Transmission . . . . .	10
2.4. Finding the C-parameters in this System . . . . .	11
2.5. Analysis . . . . .	13
2.5.1. Solving Intrinsic Impedance . . . . .	13
2.5.2. Solving Phase Constant . . . . .	17
2.5.3. Combining Solutions . . . . .	19
3. DETECTION OF BRANCHES . . . . .	21
4. COMPENSATION OF BRANCHES IN DPS METAMATERIALS . . . . .	24
4.1. Sign Branch of Wave Propagation . . . . .	24
4.2. Argument Branch of Refractive Index . . . . .	25

5. COMPENSATION OF BRANCHES IN ALL METAMATERIALS AND MATLAB COD- ING . . . . .	27
5.1. Simulation vs. Theory . . . . .	27
5.2. DPS Adjustments . . . . .	29
5.3. ENG and MNG Adjustments . . . . .	32
5.4. DNG Adjustments . . . . .	33
6. RESULTS . . . . .	35
7. CONCLUSION . . . . .	42
7.1. Future Work . . . . .	42
REFERENCES . . . . .	43
APPENDIX . . . . .	46
A.1. SParam.m . . . . .	46
A.2. CParam.m . . . . .	48
A.3. phase_tracking.m . . . . .	50

# LIST OF TABLES

<u>Table</u>	<u>Page</u>
5.1. Sampled value pairs of $\varepsilon$ and $\mu$ used for simulations. Every combination of $\pm$ was used to test each quadrant of metamaterials. Value pairs were chosen by radius 12 and various angles on the metamaterial chart ( $\angle \approx 45 \pm \{0, 5, 25\}$ ). . . . .	27
5.2. Metamaterial C-parameter characteristic chart. As the signs of $\varepsilon$ and $\mu$ change, there is corresponding signs for $Z$ and $n$ according to the equations listed above. . . . .	29
6.1. Average performance times and max error for various tests on a Intel I3-4170 (3.70GHz, Dual Core) with 12 GB of RAM and Windows 10 (ver. 1803). Note that the only tests that will use <b>sym()</b> are tests detecting ENG or MNG ( $X > 1$ ). Error is calculated as the mean of absolute value of percent difference per simulation with the max error per simulation set shown. * <i>Mean over whole set.</i> . . . . .	35



# LIST OF FIGURES

Figure	Page
1.1. Diagram of system . . . . .	2
1.2. Diagram of coordinate system . . . . .	3
2.1. Signals within the system . . . . .	6
3.1. Natural Log of Complex Exponential. As $\theta$ increases, $\text{Im}[\ln(e^{j\theta})]$ , or $\text{Arg}(e^{j\theta})$ , follows linearly until $\theta = \pi$ , for the first argument branch. . . . .	21
3.2. Derivation of $\varepsilon_r$ from S-parameters from HFSS simulation using equations listed in section 2.5.3. when $\varepsilon_r = 12.8$ and $\mu_r = 1.25$ . For a period, $\varepsilon_r$ is 12.8 as expected, until 3.75 [GHz] when a branch occurs. . . . .	22
4.1. Imaginary part of wave propagation (solid) and real part of index of refraction (dashed) plotted over frequency without any branch compensation. $e^{\gamma_{2d}}$ was derived using Eqn. (4.2) and (2.36b) and $n_2$ using (4.3). . . . .	25
4.2. $\varepsilon_r$ with various branch compensations. * shows $\varepsilon_r$ without any compensations, o shows just sign branch compensation, and $\triangle$ shows both sign and logarithmic branch compensation. . . . .	26
5.1. These value pair of $\varepsilon$ and $\mu$ were chosen for simulation and analysis. There are 5 points in each quadrant, with a constant magnitude of 12 from the center and angles of about $45 \pm \{0, 5, 25\}$ . Points are numbered 1 - 20 counter-clockwise for reference. . . . .	28
5.2. Imaginary part of the wave propagation. Sign of this is sporadic due to the inconsistent sign of $\text{imag}(X^2 - 1)$ , which is very small and prone to error. . . . .	29
5.3. Peaks shown of $\phi_n$ , the normalized phase, using the findpeaks() function of MATLAB when comparing $\phi_n$ to 1.5 as a reference point for detecting sign branches. . . . .	30
6.1. Results of deriving $\varepsilon$ from HFSS simulations based on data from Table 5.1 and Fig. 5.1 using automated phase tracking for branch compensation. The solid line (—) is the phase tracking results and dashed line (- - -) is the expected value. Each title denotes the quadrant (Q) and point (P) of MTM based on Fig. 5.1. . . . .	36
6.2. Results of deriving $\mu$ from HFSS simulations based on data from Table 5.1 and Fig. 5.1 using automated phase tracking for branch compensation. The solid line (—) is the phase tracking results and dashed line (- - -) is the expected value. Each title denotes the quadrant (Q) and point (P) of MTM based on Fig. 5.1. . . . .	37
6.3. Error of Index of Refraction in ENG at point 3 of HFSS simulation. Error is likely due to the sensitivity of X increasing with frequency. . . . .	38

6.4. Results of deriving $\varepsilon$ with phase tracking method using S-parameters from MATLAB simulation given $\varepsilon = 8 + 5\sin(f/1e9)$ and $\mu = 3$ . . . . .	38
6.5. Results of deriving $\mu$ with phase tracking method using S-parameters from MATLAB simulation given $\varepsilon = 8 + 5\sin(f/1e9)$ and $\mu = 3$ . . . . .	39
6.6. Results of deriving $\varepsilon$ with phase tracking method using S-parameters from MATLAB simulation given $\varepsilon = 8 + 5\sin(f/1e9)$ and $\mu = 5 + 3\cos(f/1e9)$ . Code produces bad branch choices after 12.24 [GHz]. . . . .	40
6.7. Results of deriving $\varepsilon$ with phase tracking method using S-parameters from MATLAB simulation given $\varepsilon = 8(1 - f/1e10) + 4\sin(f/2e9)$ and $\mu = 2$ . Note that $\varepsilon$ is crossing $\varepsilon = 0$ once, thus changing the metamaterial quadrant mid simulation. . . . .	40
6.8. Results of deriving $\varepsilon$ with phase tracking method using S-parameters from MATLAB simulation given $\varepsilon = 8(1 - f/1e10) + 1 + 4\sin(f/2e9)$ and $\mu = 2$ . Note that $\varepsilon$ is crossing $\varepsilon = 0$ 3 times, thus changing the metamaterial quadrant mid simulation but showing errors. . . . .	41

## LIST OF ABBREVIATIONS

C-parameters .....	Constitutive parameters of DEM ( $\varepsilon, \mu, \sigma$ )
DEM .....	Dielectric material
DPS .....	Double positive metamaterial
DNG .....	Double negative metamaterial
EM .....	Electromagnetic
ENG .....	Permittivity ( $\varepsilon$ ) negative metamaterial
MTM .....	Metamaterial(s)
MNG .....	Permeability ( $\mu$ ) negative metamaterial
S-parameters .....	Scattering parameters of signal normal to DEM ( $S_{11}, S_{21}$ )

# LIST OF SYMBOLS

$\alpha$	—	..... Attenuation constant, page 13
$\beta$	(rad/m)	..... Phase constant, page 12
$\varepsilon$	(F/m)	..... Permittivity, page 1
$\varepsilon_0$	(F/m)	..... Permittivity of freespace [ $\frac{1}{\mu_0 c^2}$ (F/m)], page 4
$\varepsilon_r$	—	..... Relative permittivity, page 20
$\Gamma$	—	..... Reflection coefficient, page 3
$\gamma$	—	..... Propagation constant, page 5
$\Gamma_{12}$	—	..... Reflection coefficient at front boundary of DEM, page 3
$\Gamma_{sys}$	—	..... Reflection coefficient of the system, page 3
$\Gamma_{xy}$	—	..... Local reflection off of medium $y$ into medium $x$ , page 5
$\lambda$	(m)	..... Wavelength of signal, page 4
$\mu$	(H/m)	..... Permittivity, page 1
$\mu_0$	(H/m)	..... Permeability of freespace [ $4\pi * 10^{-7}$ (H/m)], page 4
$\mu_r$	—	..... Relative permeability, page 20
$\omega$	(rad/s)	..... Angular frequency of signal, page 4
$\sigma$	(S/m)	..... Conductivity, page 1
$c$	(m/s)	..... Speed of light in vacuum [299 792 458 (m/s)], page 4
$d$	(m)	..... DEM depth, page 2
$e$	—	..... Natural number, page 5

$h$	(m) .....	DEM height, page 2
$n$	— .....	Refractive index, page 19
$S_{11}$	— .....	System Reflection, page 1
$S_{21}$	— .....	System Transmission, page 1
$T$	— .....	Transmission coefficient, page 3
$T_{sys}$	— .....	Transmission coefficient of system, page 3
$T_{xy}$	— .....	Local transmission from medium $y$ into medium $x$ , page 5
$w$	(m) .....	DEM width, page 2
$Y$	— .....	Arbitrary variable for solution of reflection coefficient, page 16
$Z$	( $\Omega$ ) .....	Intrinsic impedance, page 12
$Z_0$	( $\Omega$ ) .....	Intrinsic impedance of freespace ( $\approx 377\Omega$ ), page 12
$Z_r$	— .....	Intrinsic impedance relative to freespace ( $Z_0$ ), page 19

# 1. INTRODUCTION

## 1.1. Context

In the field of applied electromagnetics, engineers study how electromagnetic waves interact with and propagate through various materials. All materials have these three associated constitutive parameters: permittivity ( $\epsilon$ ), permeability ( $\mu$ ), and conductivity ( $\sigma$ ). Permittivity defines how an electromagnetic wave is electrically influenced by a material; permeability defines how an electromagnetic wave is magnetically influenced by a material; and conductance defines how an electromagnetic wave is absorbed by a material.

Natural materials such as copper, water, and air have their own given values for these constitutive parameters (C-parameters). However, human made materials such as ferrites and FR-4, which is a common substrate made with fiberglass cloth and an epoxy resin, can have varied C-parameters[1]. This variance can be seen across different manufacturers, different batches, when deformation or aging occurs, or at different operating frequencies.

In the studies of human made materials, all possible variations of metamaterials are being considered to optimize electronics. Metamaterials are generally considered as any material that can have a changing or negative C-parameter. Examples are the split ring resonator[2, 3] and magneto-responsive particles[4]. Metamaterials like the particles have been shown to be able to tune antennas without changing their aperture[4, 5, 6]. Tuning can mean changing the phase, operating frequency or even the beam angle of a signal from an antenna.

Several common methods to determine the permittivity of a given material are using a dielectric probe, which requires contact with the material, or measuring the scattering parameters (S-parameters) around the material. When it comes to metamaterials, using the S-parameters is often the preferred method due to their composite nature.

## 1.2. Previous Work

When using the S-parameters to determine the C-parameters, there are plenty of publications on the mathematics of how this works[7, 8, 9, 10, 11, 12, 13, 14]. One of the most iconic methods is the Nicolson-Ross-Weir method[7] developed in the 1970's and is foundational to many modern adaptations on that method. However, it was not optimized to handle synthetic materials

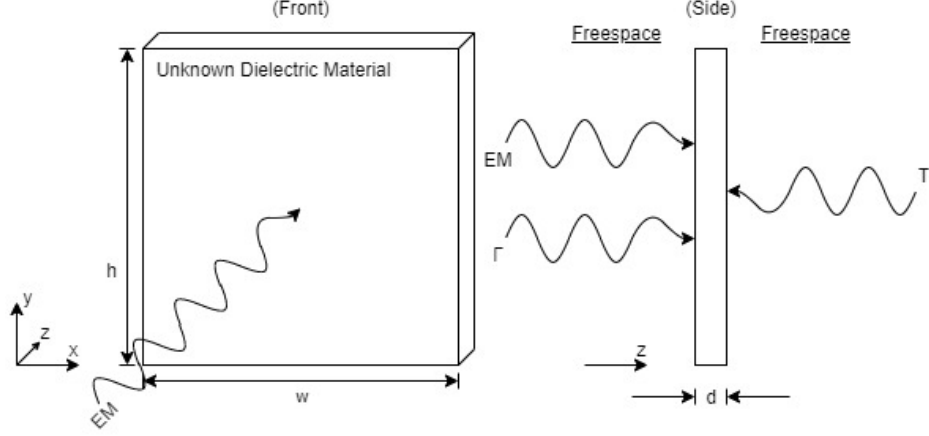


Figure 1.1. Diagram of system

with unusual electrical characteristics. Modern adaptations of the Nicolson-Ross-Weir method often use estimations or approximations to account for mathematical discontinuities or anomalies, also known as branches, which may be considered a consequence of signal resonance within a structure. However, current literature on branches are vague and do not fully explain the reason branches exist.

This thesis presents a full derivation of the Nicolson-Ross-Weir method from the boundary conditions and provides a novel method of branch detection and compensation, all accounting for the material possibly being in any metamaterial quadrant and varying with frequency and avoiding estimations or predictions in relation to the branches.

### 1.3. Setup

This question is based on a book example in [15] Section 5.5.1. If we have a dielectric slab surrounded by free space and transmit a signal normal to the surface of the slab, there will be two signals scattered from the system: a reflection signal from the front of the material moving back to the source, and a transmission signal from the back of the material moving away from the source. Measuring these two signals as the S-parameters, how can we determine the value of the dielectric material's (DEM) electrical permittivity? This concept is illustrated in Fig. 1.1.

In most other systems, the reflection ( $\Gamma_{sys}$ ) would simply be a single signal with power  $P_{Reflected} = P_{Transmitted} * \Gamma_{12}$ , where  $\Gamma_{12}$  is the reflection coefficient of a signal propagating in an outside medium (medium 1) toward the source from the material of interest (medium 2), as shown in Fig. 1.2. However, in the case where thickness,  $d$ , of the DEM is small (less than six

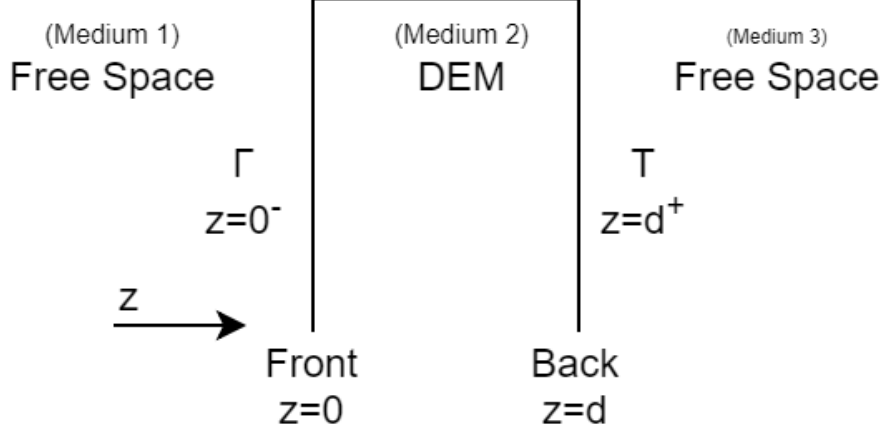


Figure 1.2. Diagram of coordinate system

wavelengths), there will be at least one more reflection off the back boundary toward the source in the  $-z$  direction. By assigning the front boundary of the DEM as the origin of the coordinate system ( $z = 0$ ), the back boundary at  $z = d$ , we can measure  $\Gamma_{sys}$  just outside the boundary at  $z = 0^-$  and  $T_{sys}$  just outside the back boundary at  $z = d^+$ .

#### 1.4. Assumptions

The following lists major assumptions that uniquely identify this system:

I *Normal incidence*. The input signal is traveling in the  $+z$  direction and encounters the slab with normal incidence ( $90^\circ$  to surface of DEM).

II *Dielectric*. Electrical conductivity is negligible; therefore

$$\sigma = 0. \quad (1.1)$$

III *Lossless*. The power reflected and the power transmitted through the material should add to the power of the original signal transmitted; therefore,

$$1 + S_{11} = S_{21}, \quad (1.2)$$

$$\alpha = 0. \quad (1.3)$$



IV *Electrically large.* Assume the slab height ( $h$ ) and width ( $w$ ) go to infinity, which is physically defined as greater than 6 wavelengths, or

$$h \approx \infty [\text{m}] > 6\lambda \quad (1.4\text{a})$$

$$w \approx \infty [\text{m}] > 6\lambda, \quad (1.4\text{b})$$

where  $\lambda$  is wavelength.

V *Homogeneous.* Assume the DEM is homogeneous, meaning the C-parameters are consistent throughout the material.

The system reflection and transmission will also be defined to be their respective scattering parameters, shown as

$$\Gamma_{sys} = S_{11} \quad (1.5\text{a})$$

$$T_{sys} = S_{21}. \quad (1.5\text{b})$$

It should also be noted that the S-parameters will be treated in their Cartesian form ( $X + jY$ ), not a decibel and phase form.

## 2. DERIVING EQUATIONS FROM BOUNDARY CONDITIONS

### 2.1. Signals

Since there are multiple internal reflections within the DEM, further denoted as "local reflections", and the DEM also has a total reflection, the total reflection coefficient of the system will be denoted as  $\Gamma_{sys}$  and the smaller reflection coefficients at the boundaries will be denoted as  $\Gamma_{xy}$  where  $x$  is the medium the signal reflects into and  $y$  is the medium the signal reflected off of. The same case also applies to transmissions  $T_{sys}$  and  $T_{xy}$ .

Every time a signal encounters a boundary, a reflection signal and a transmission signal are created. The value of the reflection and transmission coefficients depends on the C-parameters of the two mediums which define the boundary. Figure 2.1, demonstrates the process of a driving electromagnetic (EM) signal and how the local reflection and transmission signals are created.

An incident EM wave is introduced to the system and interacts with 3 mediums, each with their own C-parameters. When the EM signal encounters the front boundary between mediums 1 and 2 at  $z = 0$  it splits into two signals, a reflected signal and a transmitted signal. The reflected signal is multiplied by the reflection coefficient  $\Gamma_{12}$ , and the transmitted signal is multiplied by the transmission coefficient  $T_{21}$ . The reflected signal leaves the system and is called  $\Gamma_0$ . The transmitted signal propagates through medium 2 and is multiplied by the wave propagation,  $e^{\gamma d}$ , where  $e$  is the natural number,  $\gamma$  is the propagation constant and  $d$  is the distance propagated, which is the thickness of the material.

When the propagating signal encounters the back boundary of medium 2 with medium 3 at  $z = d$ , another set of reflected and transmitted signals are created. The transmitted signal is multiplied by  $T_{32}$ , then leaves the system through medium 3, and is called  $T_1$ . The reflected signal however stays in medium 2 and is multiplied by  $\Gamma_{23}$ . This signal then propagates through medium 2 back to  $z = 0$  and is again multiplied by  $e^{\gamma d}$ . This cycle continues with the evanescent signal inside the material reflecting back and forth, losing energy to the transmitted signals on both sides of medium 2.

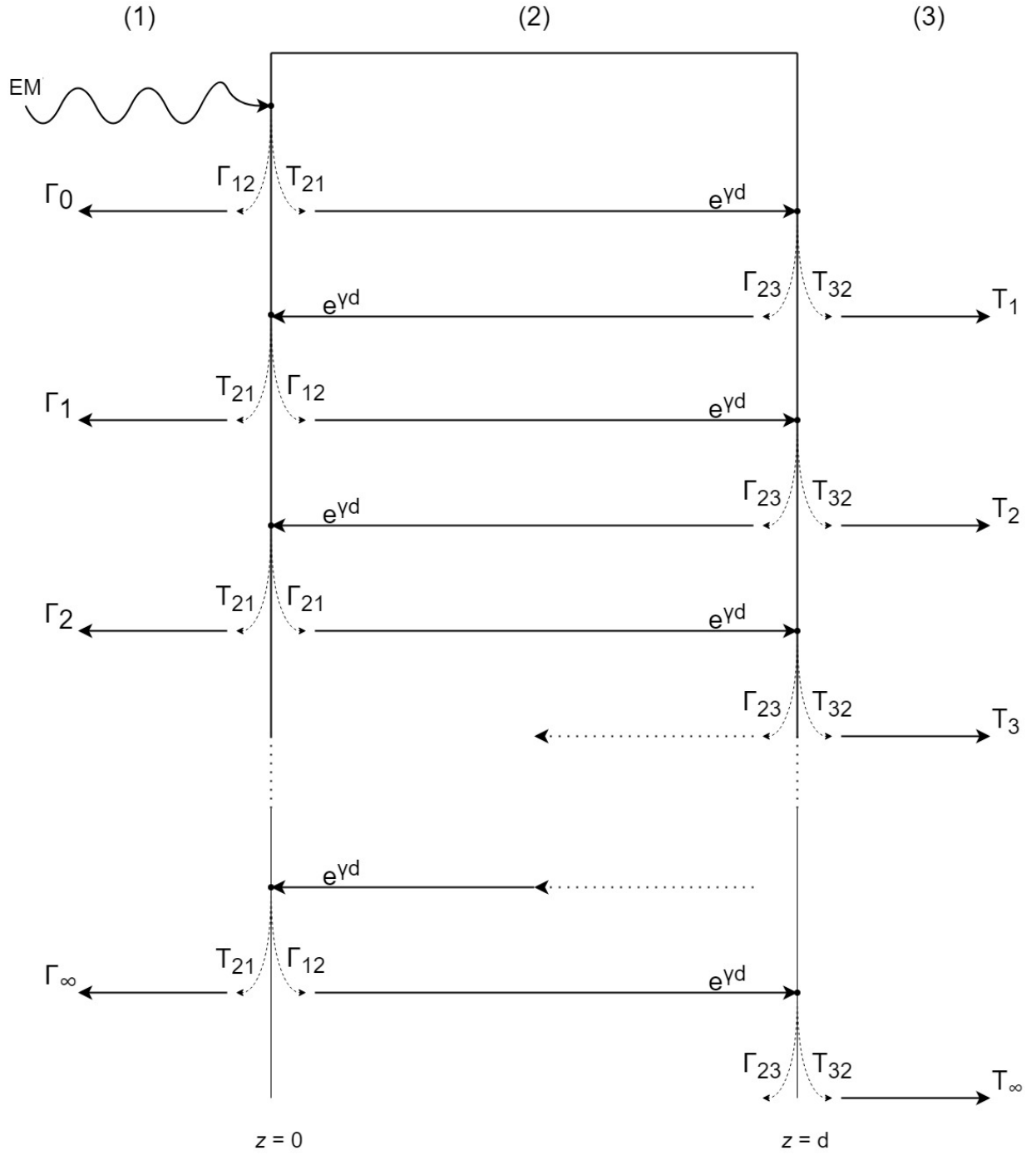


Figure 2.1. Signals within the system

## 2.2. Derivation of System Reflection

Figure 2.1, shows infinite reflections ( $\Gamma_n$  as  $n \rightarrow \infty$ ) emitted from the system. These reflections add up to make

$$\sum_{n=0}^{\infty} \Gamma_n = \Gamma_{sys}. \quad (2.1)$$

Looking at Fig. 2.1,

$$\Gamma_0 = \Gamma_{12} \quad (2.2a)$$

$$\begin{aligned} \Gamma_1 &= T_{21}e^{\gamma d}\Gamma_{23}e^{\gamma d}T_{32} \\ &= T_{21}T_{32}\Gamma_{23}e^{2\gamma d} \end{aligned} \quad (2.2b)$$

$$\begin{aligned} \Gamma_2 &= T_{21}e^{\gamma d}\Gamma_{23}e^{\gamma d}\Gamma_{21}e^{\gamma d}\Gamma_{23}e^{\gamma d}T_{32} \\ &= T_{21}T_{32}\Gamma_{21}\Gamma_{23}^2e^{4\gamma d} \end{aligned} \quad (2.2c)$$

...

$$\Gamma_n = T_{21}T_{32}\Gamma_{21}^{n-1}\Gamma_{23}^ne^{2n\gamma d} \quad (2.2d)$$

Since mediums 1 and 3 are the same the following two relations are true,

$$\Gamma_{23} = \Gamma_{21} \quad (2.3a)$$

and,

$$T_{32} = T_{12}. \quad (2.3b)$$

Therefore, equations (2.2b)-(2.2d) can be rewritten as,

$$\Gamma_1 = T_{12}T_{21}\Gamma_{21}e^{2\gamma d} \quad (2.4a)$$

$$\Gamma_2 = T_{12}T_{21}\Gamma_{21}^3e^{4\gamma d} \quad (2.4b)$$

$$\begin{aligned} \Gamma_n &= T_{12}T_{21}\Gamma_{21}^{2n-1}e^{2n\gamma d} \\ &= T_{12}T_{21}\Gamma_{21}e^{2\gamma d}(\Gamma_{21}^2e^{2\gamma d})^{n-1}. \end{aligned} \quad (2.4c)$$

Substituting Eqn. (2.2a) and Eqn. (2.4c) to Eqn. (2.1) gives the infinite series

$$\begin{aligned}
\Gamma_{sys} &= \sum_{n=0}^{\infty} \Gamma_n \\
&= \Gamma_0 + \sum_{n=1}^{\infty} \Gamma_n \\
&= \Gamma_{12} + \sum_{n=1}^{\infty} T_{12}T_{21}\Gamma_{21}e^{2\gamma d}(\Gamma_{21}^2e^{2\gamma d})^{n-1} \\
&= \Gamma_{12} + \sum_{n=0}^{\infty} T_{12}T_{21}\Gamma_{21}e^{2\gamma d}(\Gamma_{21}^2e^{2\gamma d})^n \\
&= \Gamma_{12} + T_{12}T_{21}\Gamma_{21}e^{2\gamma d} \sum_{n=0}^{\infty} (\Gamma_{21}^2e^{2\gamma d})^n.
\end{aligned} \tag{2.5}$$

For the mathematical geometric series

$$S_{\infty} = \sum_{k=0}^{\infty} r^k$$

where

$$-1 < r < 1,$$

it is known that

$$S_{\infty} = \frac{1}{1-r}.$$

Therefore, the infinite geometric sum of Eqn. (2.5) can be rewritten as

$$\sum_{n=0}^{\infty} (\Gamma_{21}^2e^{2\gamma d})^n = \frac{1}{1 - \Gamma_{21}^2e^{2\gamma d}} \tag{2.6}$$

and the whole equation can be rewritten as

$$\Gamma_{sys} = \Gamma_{12} + \frac{T_{12}T_{21}\Gamma_{21}e^{2\gamma d}}{1 - \Gamma_{21}^2e^{2\gamma d}}. \tag{2.7}$$

Now there are only four different reflection and transmission coefficients here:  $\Gamma_{12}$ ,  $\Gamma_{21}$ ,  $T_{12}$ , and  $T_{21}$ . For simplicity, all of them can be rewritten in terms of  $\Gamma_{12}$ .

Balanis[15] chapter 5 shows that

$$\Gamma_{ij} = -\Gamma_{ji} \quad (2.8a)$$

and

$$\Gamma_{ij} + T_{ij} = 1 \quad (2.8b)$$

therefore

$$T_{ij} = \Gamma_{ji} + 1. \quad (2.8c)$$

With these relations the following transformations are true:

$$\Gamma_{21} = -\Gamma_{12} \quad (2.9a)$$

$$T_{12} = 1 - \Gamma_{12} \quad (2.9b)$$

$$T_{21} = 1 + \Gamma_{12}. \quad (2.9c)$$

Given Eqn. (2.9) as transformations, Eqn. (2.7) may be rewritten as,

$$\begin{aligned} \Gamma_{sys} &= \Gamma_{12} + \frac{(1 - \Gamma_{12})(1 + \Gamma_{12})(-\Gamma_{12})e^{2\gamma d}}{1 - (-\Gamma_{12})^2 e^{2\gamma d}} \\ &= \Gamma_{12} + \frac{(1 - \Gamma_{12}^2)(-\Gamma_{12})e^{2\gamma d}}{1 - \Gamma_{12}^2 e^{2\gamma d}} \\ &= \Gamma_{12} + \frac{(\Gamma_{12}^3 - \Gamma_{12})e^{2\gamma d}}{1 - \Gamma_{12}^2 e^{2\gamma d}} \\ &= \frac{\Gamma_{12}(1 - \Gamma_{12}^2 e^{2\gamma d}) + (\Gamma_{12}^3 - \Gamma_{12})e^{2\gamma d}}{1 - \Gamma_{12}^2 e^{2\gamma d}} \\ &= \frac{\Gamma_{12} - \Gamma_{12}^3 e^{2\gamma d} + \Gamma_{12}^3 e^{2\gamma d} - \Gamma_{12} e^{2\gamma d}}{1 - \Gamma_{12}^2 e^{2\gamma d}} \\ &= \frac{\Gamma_{12} - \Gamma_{12} e^{2\gamma d}}{1 - \Gamma_{12}^2 e^{2\gamma d}}, \end{aligned} \quad (2.10)$$

and rewritten in terms of S-parameters gives

$$\Gamma_{sys} = S_{11} = \frac{\Gamma_{12}(1 - e^{2\gamma d})}{1 - \Gamma_{12}^2 e^{2\gamma d}}. \quad (2.11)$$

Now  $S_{11}$  is in terms of the local reflection,  $\Gamma_{12}$ , and the wave propagation,  $e^{2\gamma d}$ . Later these two will be rewritten to solve for  $\varepsilon$  and  $\mu$ .

### 2.3. Derivation of System Transmission

The concepts here for transmissions are the same as they were for the reflections in section 2.2. In Fig. 2.1, it is shown that there are infinitely many transmissions ( $T_n$  as  $n \rightarrow \infty$ ). These transmissions when added make

$$\sum_{n=0}^{\infty} T_n = T_{sys}. \quad (2.12)$$

Looking at Fig. 2.1,

$$\begin{aligned} T_1 &= T_{21} e^{\gamma d} T_{32} \\ &= T_{21} T_{32} e^{\gamma d} \end{aligned} \quad (2.13a)$$

$$\begin{aligned} T_2 &= T_{21} e^{\gamma d} \Gamma_{23} e^{\gamma d} \Gamma_{21} e^{\gamma d} T_{32} \\ &= T_{21} T_{32} \Gamma_{21} \Gamma_{23} e^{3\gamma d} \end{aligned} \quad (2.13b)$$

...

$$T_n = T_{21} T_{32} e^{\gamma d} (\Gamma_{21} \Gamma_{23} e^{2\gamma d})^{n-1}. \quad (2.13c)$$

Applying Eqn. (2.3) as relations to Eqn. (2.13c) produces

$$T_n = T_{12} T_{21} e^{\gamma d} (\Gamma_{21}^2 e^{2\gamma d})^{n-1}. \quad (2.14)$$

Applying Eqn. (2.14) to Eqn. (2.12),

$$\begin{aligned}
T_{sys} &= \sum_{n=0}^{\infty} T_n \\
&= \sum_{n=1}^{\infty} T_{12}T_{21}e^{\gamma d}(\Gamma_{21}^2 e^{2\gamma d})^{n-1} \\
&= T_{12}T_{21}e^{\gamma d} \sum_{n=1}^{\infty} (\Gamma_{21}^2 e^{2\gamma d})^{n-1} \\
&= T_{12}T_{21}e^{\gamma d} \sum_{n=0}^{\infty} (\Gamma_{21}^2 e^{2\gamma d})^n
\end{aligned} \tag{2.15}$$

Using the concept of the geometric series on Eqn. (2.15) gives

$$T_{sys} = \frac{T_{12}T_{21}e^{\gamma d}}{1 - \Gamma_{21}^2 e^{2\gamma d}}. \tag{2.16}$$

Finally, applying Eqn. (2.9) gives

$$\begin{aligned}
T_{sys} &= \frac{(1 - \Gamma_{12})(1 + \Gamma_{12})e^{\gamma d}}{1 - \Gamma_{21}^2 e^{2\gamma d}} \\
&= \frac{(1 - \Gamma_{12}^2)e^{\gamma d}}{1 - \Gamma_{21}^2 e^{2\gamma d}},
\end{aligned} \tag{2.17}$$

and in terms of S-parameters is

$$T_{sys} = S_{21} = \frac{e^{\gamma d}(1 - \Gamma_{12}^2)}{1 - \Gamma_{21}^2 e^{2\gamma d}}. \tag{2.18}$$

## 2.4. Finding the C-parameters in this System

Now there are two major occurrences of the C-parameters in this system: the definition of the intrinsic impedance  $Z$  and the definition of the definition of the phase constant  $\beta$ ; which are, according to Balanis[15],

$$Z = \sqrt{\frac{j\omega\mu}{\sigma + j\omega\varepsilon}} \tag{2.19a}$$

$$\beta = \omega\sqrt{\mu\varepsilon} \sqrt{\frac{1}{2} \left( 1 + \sqrt{1 + \left( \frac{\sigma}{\omega\varepsilon} \right)^2} \right)}. \tag{2.19b}$$



The goal is to solve for  $\varepsilon_2$ ; that is  $\varepsilon$  of medium 2, the DEM. Apply some of the assumptions made will simplify the definitions of  $Z_2$  and  $\beta_2$ . First, applying Eqn. (1.1) gives

$$Z_2 = \sqrt{\frac{\mu_2}{\varepsilon_2}} \quad (2.20a)$$

$$\beta_2 = \omega\sqrt{\mu_2\varepsilon_2}. \quad (2.20b)$$

$Z_2$  is the intrinsic impedance of medium 2. Intrinsic impedance can be found in the definition of the reflection coefficient

$$\Gamma_{ij} = \frac{Z_j - Z_i}{Z_j + Z_i} \quad (2.21)$$

and in this case

$$\Gamma_{12} = \frac{Z_2 - Z_1}{Z_2 + Z_1}. \quad (2.22)$$

Solving Eqn. (2.22) for  $Z_2$  gives

$$\begin{aligned} \Gamma_{12}(Z_2 + Z_1) &= Z_2 - Z_1 \\ \Gamma_{12}Z_2 + \Gamma_{12}Z_1 &= Z_2 - Z_1 \\ Z_2 - \Gamma_{12}Z_2 &= Z_1 + \Gamma_{12}Z_1 \\ Z_2(1 - \Gamma_{12}) &= Z_1(1 + \Gamma_{12}) \\ Z_2 &= Z_1 \frac{1 + \Gamma_{12}}{1 - \Gamma_{12}} \end{aligned} \quad (2.23)$$

Since mediums 1 and 3 are free space,  $Z_1 = Z_3 = Z_0$ , which is the intrinsic impedance of free space.

Applying the definition of  $Z_2$  in Eqn. (2.20a) to Eqn. (2.23) gives

$$Z_2 = \sqrt{\frac{\mu_2}{\varepsilon_2}} = Z_0 \frac{1 + \Gamma_{12}}{1 - \Gamma_{12}} \quad (2.24)$$

The phase constant of medium 2,  $\beta_2$ , can be found in the definition of the wave propagation constant,  $(\gamma)$ ,

$$\gamma = \alpha - i\beta, \quad (2.25)$$

where  $\alpha$  is the attenuation constant and  $\beta$  is the phase constant, which is the imaginary portion of  $\gamma$ . Using equation 2.25 for medium 2, we can simply solve for  $\beta_2$ ,

$$\begin{aligned}\gamma_2 &= \alpha_2 - i\beta_2 \\ i\beta_2 &= \alpha_2 - \gamma_2 \\ \beta_2 &= \frac{\alpha_2 - \gamma_2}{i} \\ \beta_2 &= i(\gamma_2 - \alpha_2)\end{aligned}\tag{2.26}$$

For medium 2, the attenuation constant is negligible, as shown in Eqn. (1.3), therefore Eqn. (2.20b) is

$$\beta_2 = \omega\sqrt{\mu_2\varepsilon_2} = i\gamma_2.\tag{2.27}$$

## 2.5. Analysis

Now definitions for  $S_{11}$ ,  $S_{21}$ ,  $Z_2$ , and  $\beta_2$  have been shown to be

$$\Gamma_{sys} = S_{11} = \frac{\Gamma_{12}(1 - e^{2\gamma_2 d})}{1 - \Gamma_{12}^2 e^{2\gamma_2 d}}\tag{2.11}$$

$$T_{sys} = S_{21} = \frac{e^{\gamma_2 d}(1 - \Gamma_{12}^2)}{1 - \Gamma_{21}^2 e^{2\gamma_2 d}}\tag{2.18}$$

$$Z_2 = \sqrt{\frac{\mu_2}{\varepsilon_2}} = Z_0 \frac{1 + \Gamma_{12}}{1 - \Gamma_{12}}\tag{2.24}$$

$$\beta_2 = \omega\sqrt{\mu_2\varepsilon_2} = i\gamma_2.\tag{2.27}$$

These equations will be used as building blocks to extract  $\varepsilon_2$  from the system in terms of S-parameters and other known values. Note that there are four (4) equations listed above, with four (4) unknowns:  $\Gamma_{12}$ ,  $\gamma_2$ ,  $\mu_2$  and  $\varepsilon_2$ .

### 2.5.1. Solving Intrinsic Impedance

The intrinsic impedance can be solved in terms of knowns by solving Eqn. (2.11) for  $e^{\gamma_2 d}$ , substituting into Eqn. (2.18), solving for  $\Gamma_{12}$ , and finally substituting into Eqn. (2.24).

First, solving Eqn. (2.11) for  $e^{\gamma_2 d}$ ,

$$\begin{aligned}
S_{11} &= \frac{\Gamma_{12}(1 - e^{2\gamma_2 d})}{1 - \Gamma_{12}^2 e^{2\gamma_2 d}} \\
S_{11}(1 - \Gamma_{12}^2 e^{2\gamma_2 d}) &= \Gamma_{12}(1 - e^{2\gamma_2 d}) \\
S_{11} - S_{11}\Gamma_{12}^2 e^{2\gamma_2 d} &= \Gamma_{12} - \Gamma_{12}e^{2\gamma_2 d} \\
\Gamma_{12}e^{2\gamma_2 d} - S_{11}\Gamma_{12}^2 e^{2\gamma_2 d} &= \Gamma_{12} - S_{11} \\
e^{2\gamma_2 d}(\Gamma_{12} - S_{11}\Gamma_{12}^2) &= \Gamma_{12} - S_{11} \\
e^{2\gamma_2 d} &= \frac{\Gamma_{12} - S_{11}}{\Gamma_{12} - S_{11}\Gamma_{12}^2} \\
e^{\gamma_2 d} &= \pm \sqrt{\frac{\Gamma_{12} - S_{11}}{\Gamma_{12} - S_{11}\Gamma_{12}^2}}
\end{aligned} \tag{2.29}$$

Now substituting Eqn. (2.29) in (2.18) and solving for  $\Gamma_{12}$ ,

$$\begin{aligned}
S_{21} &= \frac{e^{\gamma_2 d}(1 - \Gamma_{12}^2)}{1 - \Gamma_{21}^2 e^{2\gamma_2 d}} \\
S_{21} &= \pm \sqrt{\frac{\Gamma_{12} - S_{11}}{\Gamma_{12} - S_{11}\Gamma_{12}^2}} \frac{1 - \Gamma_{12}^2}{1 - \Gamma_{21}^2 \left( \frac{\Gamma_{12} - S_{11}}{\Gamma_{12} - S_{11}\Gamma_{12}^2} \right)} \\
S_{21} &= \pm \sqrt{\frac{\Gamma_{12} - S_{11}}{\Gamma_{12} - S_{11}\Gamma_{12}^2}} \frac{1 - \Gamma_{12}^2}{1 - \frac{\Gamma_{12}^2 - S_{11}\Gamma_{12}}{1 - S_{11}\Gamma_{12}}} \\
S_{21} &= \pm \sqrt{\frac{\Gamma_{12} - S_{11}}{\Gamma_{12} - S_{11}\Gamma_{12}^2}} \frac{1 - \Gamma_{12}^2}{\frac{1 - S_{11}\Gamma_{12} - \Gamma_{12}^2 + S_{11}\Gamma_{12}}{1 - S_{11}\Gamma_{12}}} \\
S_{21} &= \pm \sqrt{\frac{\Gamma_{12} - S_{11}}{\Gamma_{12} - S_{11}\Gamma_{12}^2}} \frac{(1 - \Gamma_{12}^2)(1 - S_{11}\Gamma_{12})}{1 - S_{11}\Gamma_{12} - \Gamma_{12}^2 + S_{11}\Gamma_{12}} \\
S_{21} &= \pm \sqrt{\frac{\Gamma_{12} - S_{11}}{\Gamma_{12} - S_{11}\Gamma_{12}^2}} \frac{(1 - \Gamma_{12}^2)(1 - S_{11}\Gamma_{12})}{1 - \Gamma_{12}^2} \\
S_{21} &= \pm \sqrt{\frac{\Gamma_{12} - S_{11}}{\Gamma_{12} - S_{11}\Gamma_{12}^2}} (1 - S_{11}\Gamma_{12}) \\
S_{21}^2 &= \frac{\Gamma_{12} - S_{11}}{\Gamma_{12} - S_{11}\Gamma_{12}^2} (1 - S_{11}\Gamma_{12})^2 \\
S_{21}^2 &= \frac{\Gamma_{12} - S_{11}}{\Gamma_{12}(1 - S_{11}\Gamma_{12})} (1 - S_{11}\Gamma_{12})^2 \\
S_{21}^2 &= \frac{\Gamma_{12} - S_{11}}{\Gamma_{12}} (1 - S_{11}\Gamma_{12}) \\
S_{21}^2 \Gamma_{12} &= (\Gamma_{12} - S_{11})(1 - S_{11}\Gamma_{12}) \\
S_{21}^2 \Gamma_{12} &= \Gamma_{12} - S_{11} - S_{11}\Gamma_{12}^2 + S_{11}^2 \Gamma_{12} \\
0 &= S_{11}\Gamma_{12}^2 + S_{21}^2 \Gamma_{12} - S_{11}^2 \Gamma_{12} - \Gamma_{12} + S_{11} \\
0 &= \Gamma_{12}^2 (S_{11}) + \Gamma_{12} (S_{21}^2 - S_{11}^2 - 1) + (S_{11}) \\
0 &= \Gamma_{12}^2 \left( \frac{1}{2} \right) + \Gamma_{12} \left( \frac{S_{21}^2 - S_{11}^2 - 1}{2S_{11}} \right) + \left( \frac{1}{2} \right) \\
\Gamma_{12} &= \frac{1 + S_{11}^2 - S_{21}^2}{2S_{11}} \pm \sqrt{\left( \frac{S_{21}^2 - S_{11}^2 - 1}{2S_{11}} \right)^2 - 1} \\
\Gamma_{12} &= \frac{1 + S_{11}^2 - S_{21}^2}{2S_{11}} \pm \sqrt{\left( \frac{1 + S_{11}^2 - S_{21}^2}{2S_{11}} \right)^2 - 1}
\end{aligned} \tag{2.30}$$

A simplified form of this equation can be,

$$\Gamma_{12} = Y \pm \sqrt{Y^2 - 1} \quad (2.31a)$$

$$Y = \frac{1 + S_{11}^2 - S_{21}^2}{2S_{11}}, \quad (2.31b)$$

using  $Y$  as an arbitrary variable. Now substituting Eqn. (2.31) into Eqn. (2.24) and simplifying gives

$$\begin{aligned} Z_2 &= Z_0 \frac{1 + \Gamma_{12}}{1 - \Gamma_{12}} \\ \frac{Z_2^2}{Z_0^2} &= \left( \frac{1 + Y \pm \sqrt{Y^2 - 1}}{1 - Y \mp \sqrt{Y^2 - 1}} \right)^2 \\ &= \frac{Y^2 \pm 2Y\sqrt{Y^2 - 1} + Y^2 - 1 + 2Y \pm 2\sqrt{Y^2 - 1} + 1}{Y^2 \pm 2Y\sqrt{Y^2 - 1} + Y^2 - 1 - 2Y \mp 2\sqrt{Y^2 - 1} + 1} \\ &= \frac{2Y^2 + 2Y \pm 2Y\sqrt{Y^2 - 1} \pm 2\sqrt{Y^2 - 1}}{2Y^2 - 2Y \pm 2Y\sqrt{Y^2 - 1} \mp 2\sqrt{Y^2 - 1}} \\ &= \frac{Y^2 + Y \pm Y\sqrt{Y^2 - 1} \pm \sqrt{Y^2 - 1}}{Y^2 - Y \pm Y\sqrt{Y^2 - 1} \mp \sqrt{Y^2 - 1}} \\ &= \frac{Y(Y + 1) \pm \sqrt{Y^2 - 1}(Y + 1)}{Y(Y - 1) \pm \sqrt{Y^2 - 1}(Y - 1)} \\ &= \frac{(Y + 1)(Y \pm \sqrt{Y^2 - 1})}{(Y - 1)(Y \pm \sqrt{Y^2 - 1})} \\ &= \frac{Y + 1}{Y - 1} \\ &= \frac{\frac{1 + S_{11}^2 - S_{21}^2}{2S_{11}} - 1}{\frac{1 + S_{11}^2 - S_{21}^2}{2S_{11}} + 1} \\ &= \frac{\frac{1 + S_{11}^2 - S_{21}^2 - 2S_{11}}{2S_{11}}}{\frac{1 + S_{11}^2 - S_{21}^2 + 2S_{11}}{2S_{11}}} \\ &= \frac{1 + S_{11}^2 - S_{21}^2 - 2S_{11}}{1 + S_{11}^2 - S_{21}^2 + 2S_{11}} \\ &= \frac{1 - 2S_{11} + S_{11}^2 - S_{21}^2}{1 + 2S_{11} + S_{11}^2 - S_{21}^2} \\ &= \frac{(1 - S_{11})^2 - S_{21}^2}{(1 + S_{11})^2 - S_{21}^2}. \end{aligned} \quad (2.32)$$

Now  $Z_2$  is completely in terms of knowns as

$$Z_2 = \sqrt{\frac{\mu_2}{\varepsilon_2}} = \pm Z_0 \sqrt{\frac{S_{21}^2 - (1 + S_{11})^2}{S_{21}^2 - (1 - S_{11})^2}}. \quad (2.33)$$

### 2.5.2. Solving Phase Constant

The method to solving the phase constant in terms of knowns will be similar to the last section. First solve Eqn. (2.18) for  $\Gamma_{12}$ , substitute into Eqn. (2.11), solve for  $e^{\gamma_2 d}$ , solve for  $\gamma_2$ , and finally substitute into equation 2.27.

First, solve Eqn. (2.18) for  $\Gamma_{12}$  as

$$\begin{aligned} S_{21} &= \frac{e^{\gamma_2 d}(1 - \Gamma_{12}^2)}{1 - \Gamma_{12}^2 e^{2\gamma_2 d}} \\ (1 - \Gamma_{12}^2 e^{2\gamma_2 d})S_{21} &= e^{\gamma_2 d}(1 - \Gamma_{12}^2) \\ S_{21} - S_{21}\Gamma_{12}^2 e^{2\gamma_2 d} &= e^{\gamma_2 d} - e^{\gamma_2 d}\Gamma_{12}^2 \\ e^{\gamma_2 d}\Gamma_{12}^2 - S_{21}\Gamma_{12}^2 e^{2\gamma_2 d} &= e^{\gamma_2 d} - S_{21} \\ \Gamma_{12}^2(e^{\gamma_2 d} - S_{21}e^{2\gamma_2 d}) &= e^{\gamma_2 d} - S_{21} \\ \Gamma_{12}^2 &= \frac{e^{\gamma_2 d} - S_{21}}{e^{\gamma_2 d} - S_{21}e^{2\gamma_2 d}} \\ \Gamma_{12} &= \pm \sqrt{\frac{e^{\gamma_2 d} - S_{21}}{e^{\gamma_2 d} - S_{21}e^{2\gamma_2 d}}}. \end{aligned} \quad (2.34)$$

Now substitute this solution for  $\Gamma_{12}$  into Eqn. (2.11),

$$\begin{aligned}
S_{11} &= \frac{\Gamma_{12}(1 - e^{2\gamma_2 d})}{1 - \Gamma_{12}^2 e^{2\gamma_2 d}} \\
\Gamma_{12} &= \left( \frac{S_{11}}{1 - e^{2\gamma_2 d}} \right) (1 - \Gamma_{12}^2 e^{2\gamma_2 d}) \\
\pm \sqrt{\frac{e^{\gamma_2 d} - S_{21}}{e^{\gamma_2 d} - S_{21} e^{2\gamma_2 d}}} &= \left( \frac{S_{11}}{1 - e^{2\gamma_2 d}} \right) \left( 1 - \left( \frac{e^{\gamma_2 d} - S_{21}}{e^{\gamma_2 d} - S_{21} e^{2\gamma_2 d}} \right) e^{2\gamma_2 d} \right) \\
\pm \sqrt{\frac{e^{\gamma_2 d} - S_{21}}{e^{\gamma_2 d} - S_{21} e^{2\gamma_2 d}}} &= \left( \frac{S_{11}}{1 - e^{2\gamma_2 d}} \right) \left( 1 - \frac{e^{2\gamma_2 d} - S_{21} e^{\gamma_2 d}}{1 - S_{21} e^{\gamma_2 d}} \right) \\
\pm \sqrt{\frac{e^{\gamma_2 d} - S_{21}}{e^{\gamma_2 d} - S_{21} e^{2\gamma_2 d}}} &= \left( \frac{S_{11}}{1 - e^{2\gamma_2 d}} \right) \frac{(1 - S_{21} e^{\gamma_2 d}) - e^{2\gamma_2 d} + S_{21} e^{\gamma_2 d}}{1 - S_{21} e^{\gamma_2 d}} \\
\pm \sqrt{\frac{e^{\gamma_2 d} - S_{21}}{e^{\gamma_2 d} - S_{21} e^{2\gamma_2 d}}} &= \left( \frac{S_{11}}{1 - e^{2\gamma_2 d}} \right) \frac{1 - e^{2\gamma_2 d}}{1 - S_{21} e^{\gamma_2 d}} \\
\pm \sqrt{\frac{e^{\gamma_2 d} - S_{21}}{e^{\gamma_2 d} - S_{21} e^{2\gamma_2 d}}} &= \frac{S_{11}}{1 - S_{21} e^{\gamma_2 d}} \\
\frac{e^{\gamma_2 d} - S_{21}}{e^{\gamma_2 d} - S_{21} e^{2\gamma_2 d}} &= \frac{S_{11}^2}{(1 - S_{21} e^{\gamma_2 d})^2} \\
\frac{e^{\gamma_2 d} - S_{21}}{e^{\gamma_2 d}(1 - S_{21} e^{\gamma_2 d})} &= \frac{S_{11}^2}{(1 - S_{21} e^{\gamma_2 d})^2} \\
\frac{e^{\gamma_2 d} - S_{21}}{e^{\gamma_2 d}} &= \frac{S_{11}^2}{1 - S_{21} e^{\gamma_2 d}} \\
S_{11}^2 e^{\gamma_2 d} &= (e^{\gamma_2 d} - S_{21})(1 - S_{21} e^{\gamma_2 d}) \\
0 &= S_{21} e^{2\gamma_2 d} + S_{11}^2 e^{\gamma_2 d} - S_{21}^2 e^{\gamma_2 d} - e^{\gamma_2 d} + S_{21} \\
0 &= e^{2\gamma_2 d}(S_{21}) + e^{\gamma_2 d}(S_{11}^2 - S_{21}^2 - 1) + S_{21} \\
0 &= e^{2\gamma_2 d}\left(\frac{1}{2}\right) + e^{\gamma_2 d}\left(\frac{S_{11}^2 - S_{21}^2 - 1}{2S_{21}}\right) + \frac{1}{2} \\
e^{\gamma_2 d} &= \frac{1 + S_{21}^2 - S_{11}^2}{2S_{21}} \pm \sqrt{\left(\frac{1 + S_{21}^2 - S_{11}^2}{2S_{21}}\right)^2 - 1}.
\end{aligned} \tag{2.35}$$

A simplified form of this equation can be

$$e^{\gamma_2 d} = X \pm \sqrt{X^2 - 1} \tag{2.36a}$$

$$X = \frac{1 + S_{21}^2 - S_{11}^2}{2S_{21}}. \tag{2.36b}$$

Now solve Eqn. (2.36a) for  $\beta_2$ ,

$$\begin{aligned}
e^{\gamma_2 d} &= X \pm \sqrt{X^2 - 1} \\
\ln [e^{\gamma_2 d}] &= \ln [X \pm \sqrt{X^2 - 1}] \\
\ln |e^{\gamma_2 d}| + j \left( \arg [e^{\gamma_2 d}] + 2\pi m \right) &= \ln [X \pm \sqrt{X^2 - 1}] \\
\text{Real} [\gamma_2 d] + j (\text{Imag} [\gamma_2 d] + 2\pi m) &= \ln [X \pm \sqrt{X^2 - 1}] \\
\sigma_2 d + j (-\beta_2 d + 2\pi m) &= \ln [X \pm \sqrt{X^2 - 1}] \\
j (-\beta_2 d + 2\pi m) &= \ln [X \pm \sqrt{X^2 - 1}] \\
\beta_2 d + 2\pi m &= j \ln [X \pm \sqrt{X^2 - 1}] \\
\beta_2 d &= j \ln [X \pm \sqrt{X^2 - 1}] + 2\pi m \\
\beta_2 = \omega \sqrt{\mu_2 \varepsilon_2} &= \frac{j \ln [X \pm \sqrt{X^2 - 1}] + 2\pi m}{d},
\end{aligned} \tag{2.37}$$

where the logarithm branch  $m \in \mathbb{Z}$ . Note that this means there are infinite solutions for the phase constant as  $m$  varies. This will lead to the infamous branches later.

### 2.5.3. Combining Solutions

Now the intrinsic impedance and the phase constant are in terms of knowns in Eqn. (2.33) and (2.37). Note that the values of permittivity and permeability used are their non-relative values, near the order of  $10^{-7}$ . In order to find the relative values, the previous equations may be modified. The relative intrinsic impedance,  $Z_r$  can be defined as

$$Z_r = \frac{Z}{Z_0}, \tag{2.38}$$

thus  $Z_r$  is relative to freespace. The phase constant may also be broken down to solve for the refractive index,  $n$ , in the definition

$$\beta = \frac{\omega n}{c} \tag{2.39a}$$

$$n = \sqrt{\mu_r \varepsilon_r}. \tag{2.39b}$$



Note that this definition is valid as  $c = \frac{1}{\sqrt{\mu_0 \varepsilon_0}}$ . Thus Eqn. (2.33) and (2.37) may be rewritten as

$$Z_{2,r} = \sqrt{\frac{\mu_{2,r}}{\varepsilon_{2,r}}} = \pm \sqrt{\frac{S_{21}^2 - (1 + S_{11})^2}{S_{21}^2 - (1 - S_{11})^2}} \quad (2.40)$$

$$n_2 = \sqrt{\mu_{2,r} \varepsilon_{2,r}} = \frac{j \ln [e^{\gamma_2 d}] + 2\pi m}{\omega d / c} \quad (2.41)$$

where

$$e^{\gamma_2 d} = X \pm \sqrt{X^2 - 1} \quad (2.36a)$$

$$X = \frac{1 + S_{21}^2 - S_{11}^2}{2S_{21}}. \quad (2.36b)$$

Finally the relative C-parameters can easily be solved for by the relations

$$\varepsilon_{2,r} = n_2 / Z_{2,r} \quad (2.43a)$$

$$\mu_{2,r} = n_2 * Z_{2,r}. \quad (2.43b)$$

Now it is clearly seen that the C-parameters are solved exclusively in terms of the S-parameters, the signal frequency, DEM depth, and the logarithm branch. The rest of this thesis will tackle determining:

- The integer value used for the logarithm branch
- The sign branch in Eqn. (2.36a)
- The sign branch in Eqn. (2.40).

Though, next will be determining when branches occur.

### 3. DETECTION OF BRANCHES<sup>1</sup>

Branches in this system are defined as discontinuities, unusual jumps, or deviations in a function. In this case, the branches to be concerned about are those that occur in the function definition of permittivity. However, since permittivity has been shown to be dependent on impedance and the index of refraction, the problem of branches is likely to be found in those variables first.

In the mathematics of detecting branches, it is important not to make the simplification that  $\ln[e^{j\gamma d}] = j\gamma d$ . This equation will be valid for low frequencies, but there is a problem when  $\gamma$  has an imaginary component. For the lossless case,  $\gamma = j\omega n/c$  and  $\text{Imag}[n] = 0$ , thus it is purely imaginary.

In the case of a logarithm of a complex number there is an imaginary argument statement; or  $\log(z) = \log|z| + j(\text{Arg}[z] + 2m\pi)$ , where  $z$  is any complex number,  $\text{Arg}[z]$  is the complex angle of  $z$  modulated to the range  $(-\pi, \pi]$ , and  $m$  is any integer. This concept is represented in Fig. 3.1. The first logarithmic branch occurs when the argument of the exponential first reaches a value of  $\pm\pi$ .

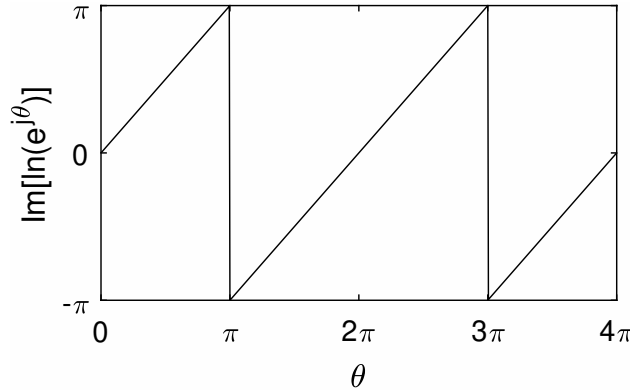


Figure 3.1. Natural Log of Complex Exponential. As  $\theta$  increases,  $\text{Im}[\ln(e^{j\theta})]$ , or  $\text{Arg}(e^{j\theta})$ , follows linearly until  $\theta = \pi$ , for the first argument branch.

<sup>1</sup>The work in this chapter is based on an article[16] published by the author of this thesis, Jacob Lewis, along with Dr. Benjamin D. Braaten, Jerika Cleveland, Dipankar Mitra, Dr. Jeffrey Allen, and Dr. Monica Allen. This team of people together derived the topic of investigation, while Jacob performed the research and wrote the majority of the article. Revisions to both theoretical and written aspects of the article were done by the whole team.

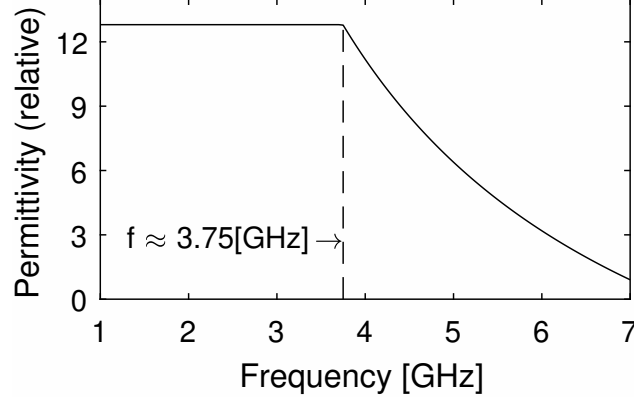


Figure 3.2. Derivation of  $\varepsilon_r$  from S-parameters from HFSS simulation using equations listed in section 2.5.3. when  $\varepsilon_r = 12.8$  and  $\mu_r = 1.25$ . For a period,  $\varepsilon_r$  is 12.8 as expected, until 3.75 [GHz] when a branch occurs.

For example, for the system in Fig. 2.1, the first branch is when  $|\gamma d| = \left|\frac{\omega nd}{c}\right| = \pi$ . Assuming  $\varepsilon_r = 12.8$ ,  $\mu_r = 1.25$ , and  $d = 0.01$  [m], the first branch would be expected when

$$\begin{aligned}
 \left|\frac{\omega nd}{c}\right| &= \pi \\
 2\pi f d |n| &= c\pi \\
 f &= \frac{c}{2d|\sqrt{\varepsilon_r \mu_r}|} \\
 f &\approx 3.75[\text{GHz}].
 \end{aligned} \tag{3.1}$$

Simulations to verify this were run in both HFSS and MATLAB, which used only equations previously listed. Figure 3.2 shows the derived permittivity from the S-parameters of a simulation in HFSS. The simulation used Floquet ports for an infinite simulated length and width of a dielectric substrate with an incident plane wave designed some distance off the boundaries of the substrate. The S-parameters were deembedded to just off the boundaries of the substrate to mitigate the substrate, as represented in Fig. 1.2. The substrate physical and electrical parameters were defined according to the example described above for comparison. It is seen that there is a variation in the permittivity at the expected frequency of 3.75 [GHz]. It has been discovered that, according the equation used to find the first branch, branches occur when the relation

$$2fdn = cm \tag{3.2}$$

is true, for any value of the integer  $m$ .

It should be noted that this branch is due to a form of resonance, based on the electrical and geometric properties of the DEM.

Another method discovered to predict branches if  $n$  is not known is to track  $e^{\gamma d}$  with Eqn. (2.36a) for when the argument of this statement reaches a value of  $\pm\pi$ . Though the argument branch has been identified and detected, it, as well as the sign branches, still need to be properly compensated.

## 4. COMPENSATION OF BRANCHES IN DPS METAMATERIALS<sup>1</sup>

Looking at the assumptions of section 1.4, a common conclusion for determining which sign to use of Eqn. (2.36a) and (2.41) is that the criteria

$$\text{Real}[Z_r] \geq 0 \tag{4.1a}$$

$$\text{Imag}[n] \geq 0 \tag{4.1b}$$

must be maintained, as negative real impedance implies a gain of power and negative imaginary refractive index implies losses. These assumptions are useful and a good starting point, but they tend to break down if  $Z_r \rightarrow 0$  or  $n \rightarrow 0$ . In the studies for this thesis, small variations have been found on both of these values. If the variations are close to 0, the variables may change signs between  $0^+$  and  $0^-$ . This concept is discussed further in the next chapter. Thus further analysis into these branches is needed to find alternative methods of sign branch selection for accurate results. For the sake of analysis, Eqn. (2.36a) will be rewritten as

$$e^{\gamma_{2d}} = X + m_1 \sqrt{X^2 - 1} \tag{4.2}$$

and Eqn. (2.41) will be rewritten as

$$n_2 = \frac{c}{\omega d} \left( \ln \left[ e^{\gamma_{2d}} \right] + 2\pi m_2 \right). \tag{4.3}$$

### 4.1. Sign Branch of Wave Propagation

If  $m_1$  is chosen by default to be positive, Eqn. (4.2) is plotted as a function of frequency. It can be seen in Fig. 4.1 that the imaginary portion has sharp changes when reaching the value zero. Interestingly, for this case of a DPS system, the two values of  $m_1$  give complex conjugates

---

<sup>1</sup>The work in this chapter is based on an article[17] published by the author of this thesis, Jacob Lewis, along with Dr. Benjamin D. Braaten, Jerika Cleveland, Dipankar Mitra, Dr. Jeffrey Allen, and Dr. Monica Allen. This team of people together derived the topic of investigation, while Jacob performed the research and wrote the majority of the article. Revisions to both theoretical and written aspects of the article were done by the whole team.

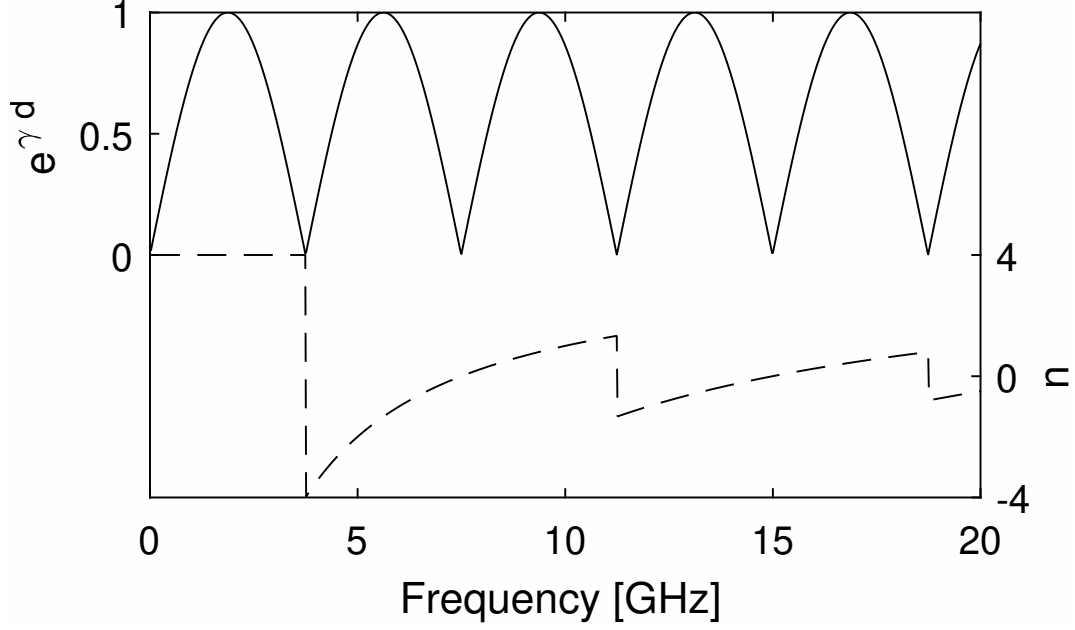


Figure 4.1. Imaginary part of wave propagation (solid) and real part of index of refraction (dashed) plotted over frequency without any branch compensation.  $e^{\gamma_2 d}$  was derived using Eqn. (4.2) and (2.36b) and  $n_2$  using (4.3).

for  $e^{\gamma_2 d}$ . It is appropriate to choose the positive branch at DC and oscillate between positive and negative each time  $\text{Imag}[e^{\gamma_2 d}] \approx 0$ . Thus the value of  $m_2$  will oscillate between +1 and -1, with a duration of approximately 3.75 [GHz] on each value for this scenario. This will result in a sign branch corrected, non-jagged sinusiod.

#### 4.2. Argument Branch of Refractive Index

Analyzing  $m_2$  of (4.3), technically there can only be one branch that provides the correct value of  $n_2$ . If  $m_2$  is chosen by default to be 0,  $n_2$  can be plotted as a function of frequency, as seen in Fig. 4.1. It can be seen that there are branch discontinuities at similar frequencies as the  $m_1$  branch changes shown in Fig. 4.1. If  $m_2$  is incremented by 1 at each of these branch frequencies, the result is a continuous value of  $n_2 = 4$ , which is the theoretically expected value from the known values of the constitutive parameters. Using the values of  $Z_r$  and  $n_2$ , Fig. 4.2 shows  $\varepsilon_r$  with and without the various branch compensations demonstrated in this thesis.

This method of branch compensation for C-parameter retrieval from the S-parameters is referenced by the author as the *phase tracking method*, as it primarily tracks the phase, or argument, over frequency. This method is effective and can be automated in MATLAB for ease and speed.

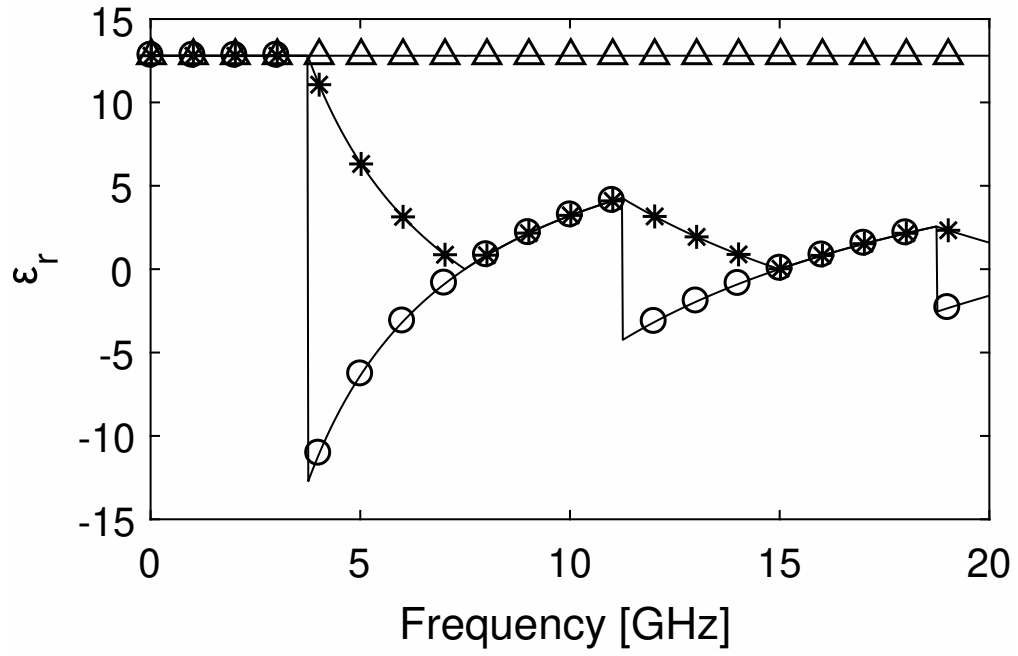


Figure 4.2.  $\epsilon_r$  with various branch compensations. \* shows  $\epsilon_r$  without any compensations, o shows just sign branch compensation, and  $\Delta$  shows both sign and logarithmic branch compensation.

## 5. COMPENSATION OF BRANCHES IN ALL METAMATERIALS AND MATLAB CODING

The theory will now be expanded to include all quadrants of metamaterials (MTM) and major challenges with automating this method in MATLAB will be identified and compensated. This chapter will use simulated data with various values of C-parameters, with the intention of using the S-parameters to derive the already known C-parameters. 20 simulations were performed with thickness  $d = 1$  [cm], frequency  $f = [1, 20]$  GHz, and varying  $\varepsilon$  and  $\mu$ . The values of  $\varepsilon$  and  $\mu$  were determined using the MTM chart with constant radius 12 and various angles to produce the value pairs shown in TABLE 5.1 and illustrated in the MTM chart in Fig. 5.1.

### 5.1. Simulation vs. Theory

Expanding the HFSS simulation to include all four quadrants of metamaterials, the simulation shows that the current theory does not match the simulation values when  $\varepsilon < 0$  (ENG & DPS). *Present simulation results vs. theoretical results deriving S-parameters.*

The current theory as it is written only will deliver a positive  $\varepsilon_r$ . When we analyze the case of DNG, it has been shown that  $n$  should be negative. However, when deriving  $n$  from  $\varepsilon_r$  and  $\mu_r$ , if both are to be negative, then their signs cancel and  $n$  remains positive. The solution to this is to separate the square root function into

$$n = \sqrt{\varepsilon_r} \sqrt{\mu_r}; \quad (5.1)$$

Table 5.1. Sampled value pairs of  $\varepsilon$  and  $\mu$  used for simulations. Every combination of  $\pm$  was used to test each quadrant of metamaterials. Value pairs were chosen by radius 12 and various angles on the metamaterial chart (  $\angle \approx 45 \pm \{0, 5, 25\}$  ).

$\pm\varepsilon$	11.9583	10.8854	8.4853	5.0505	1
$\pm\mu$	1	5.0505	8.4853	10.8854	11.9583



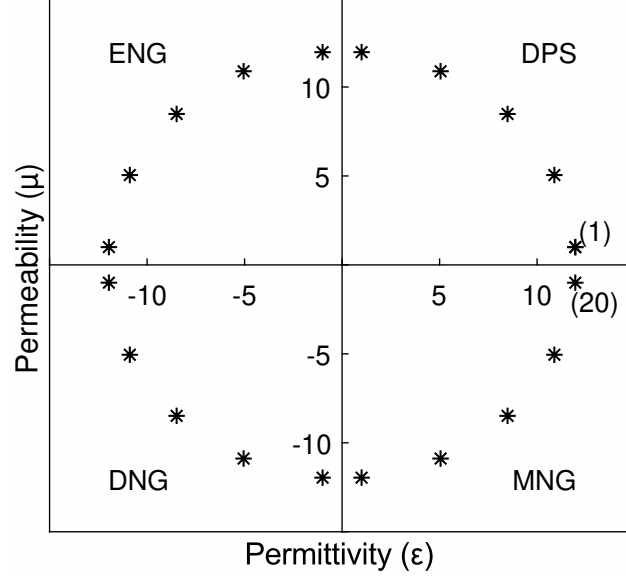


Figure 5.1. These value pair of  $\varepsilon$  and  $\mu$  were chosen for simulation and analysis. There are 5 points in each quadrant, with a constant magnitude of 12 from the center and angles of about  $45 \pm \{0, 5, 25\}$ . Points are numbered 1 - 20 counter-clockwise for reference.

which, for  $\varepsilon_{-,r} \in \varepsilon_r < 0$  and  $\mu_{-,r} \in \mu_r < 0$ , produces

$$\begin{aligned}
 n &= \sqrt{-\varepsilon_{-,r}} \sqrt{-\mu_{-,r}} \\
 &= j \sqrt{\varepsilon_{-,r}} j \sqrt{\mu_{-,r}} \\
 &= -\sqrt{\varepsilon_{-,r}} \sqrt{\mu_{-,r}},
 \end{aligned} \tag{5.2}$$

which is expected. The same also is necessary for the definition of  $Z_r$ ,

$$Z_r = \sqrt{\frac{\mu_r}{\varepsilon_r}} = \frac{\sqrt{\mu_r}}{\sqrt{\varepsilon_r}}, \tag{5.3}$$

which produces

$$Z_r = \frac{\sqrt{-\mu_{-,r}}}{\sqrt{-\varepsilon_{-,r}}} = \frac{j \sqrt{\mu_{-,r}}}{j \sqrt{\varepsilon_{-,r}}} = \frac{\sqrt{\mu_{-,r}}}{\sqrt{\varepsilon_{-,r}}}. \tag{5.4}$$

This fixes the path to the S-parameters from C-parameters; though, the same problem does not exist in solving the C-parameters from S-parameters. This table illustrates the relationship between  $(\varepsilon_r, \mu_r)$  and  $(n, Z_r)$  with the new definitions, which are shown in Table 5.2.

Table 5.2. Metamaterial C-parameter characteristic chart. As the signs of  $\varepsilon$  and  $\mu$  change, there is corresponding signs for  $Z$  and  $n$  according to the equations listed above.

$\varepsilon$	$\mu$	$Z$	$n$
+	+	+	+
-	+	$-j$	$+j$
-	-	+	-
+	-	$+j$	$+j$

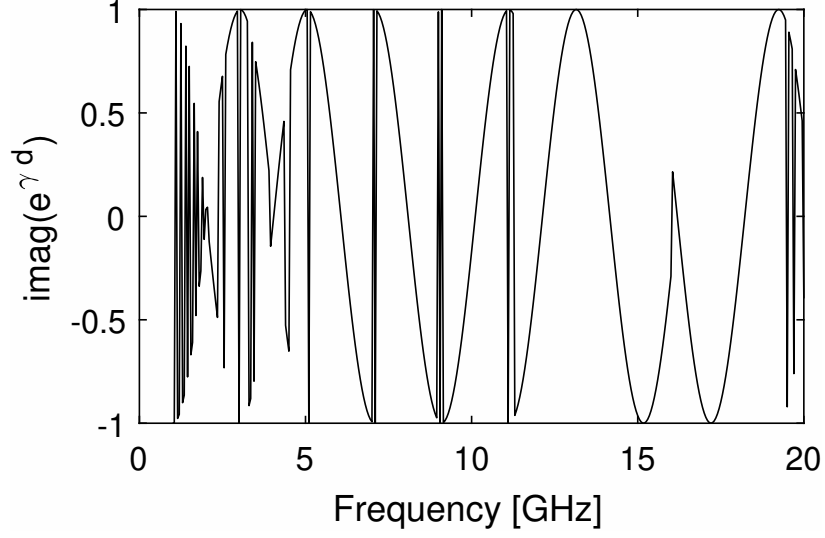


Figure 5.2. Imaginary part of the wave propagation. Sign of this is sporadic due to the inconsistent sign of  $\text{imag}(X^2 - 1)$ , which is very small and prone to error.

## 5.2. DPS Adjustments

For double positive systems (DPS), an issue is present in calculating the wave propagation.  $\sqrt{X^2 - 1}$  is easily sporadic, due to the fact that  $X$  has been found to be real and less than 1, thus  $X^2 - 1$  will be negative. However, if there is any level of an imaginary component in  $X$ , due to rounding errors, the sign will determine if the root has an angle of  $\pm\pi$ . This is shown in Fig. 5.2. [8] showed the equation for the wave propagation to be

$$e^{\gamma d} = X \pm j\sqrt{1 - X^2} \quad (5.5)$$

which alleviates the issue of the unstable sign of the imaginary portion of the wave propagation.

Another solution is to eliminate the imaginary portion of  $X$ . It has been found that for lossless MTM,  $X$  is almost purely real at all times. The imaginary portion can be neglected and

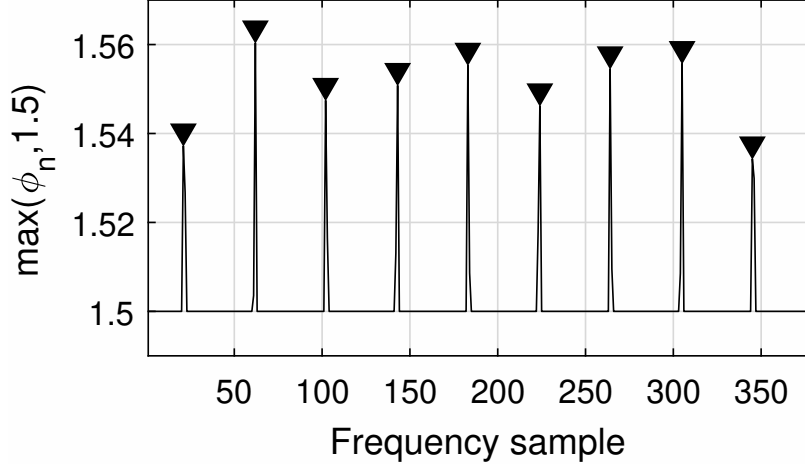


Figure 5.3. Peaks shown of  $\phi_n$ , the normalized phase, using the `findpeaks()` function of MATLAB when comparing  $\phi_n$  to 1.5 as a reference point for detecting sign branches.

assumed to be from calculation and rounding errors. This solution will be used for the remainder of this paper as it applies to all quadrants of MTM with no noticeable loss of information. However, it should be further investigated as to why  $X$  is real when it is based on the complex values of the S-parameters.

The second issue to address in automating is the branch compensations, which were well described in [17]. One assumption used for solving C-parameters is that  $\text{imag}(n) > 0$ . However, for DPS,  $\text{imag}(n) \approx 0$ , therefore choosing the proper sign branch of  $e^{\gamma d}$  requires tracking the phase. In this case, sign branches occur when the phase  $\gamma d = \{0, \pi\}$ , which calculated by taking the angle of  $e^{\gamma d}$  in MATLAB. Due to sampling issues, sampling greater frequencies will allow for more precise locations and compensations of sign branches. Since at this point the phase will be oscillating between 0 and  $\pi$ , a recommended method is to normalize the phase by using

$$\phi_n = \left| \phi - \frac{\pi}{2} \right| \quad (5.6)$$

where  $\phi$  is the phase  $\gamma d$  and  $\phi_n$  is the normalized phase. This method will allow all sign branches to be at peaks in the curve above 1.5 [rad]. This concept is illustrated in Fig. 5.3 and the code is shown in Listing 5.1. `phi` is  $\phi$ , an array over frequency, `findpeaks()` is a MATLAB function in the Signal Processing Toolbox, and `m1` is the sign branch array. Notice that the code only looks for peaks above 1.5 in `phi`, and assigns their location to the variable `pks`. The `pks` element(s) of `m1` are

Listing 5.1. MATLAB code for sign branches

```

1  phi = angle(pro);
2  phin = abs(phi-pi/2);
3  [~, pks] = findpeaks(max(phin,1.5));
4  m1(pks) = -1;
5  m1 = cumprod(m1);

```

Listing 5.2. MATLAB code for log branches

```

1  phi = angle(pro);
2  [~, pks] = findpeaks(max(phi,3));
3  val = phi(pks - 1) > 0;
4  m2(pks + val) = val*2 - 1;
5  m2 = cumsum(m2);

```

then assigned to -1, to represent an inflection in the branch array. The array is then cumulatively multiplied to carry the sign changes throughout. `m1` was initialized as an array of ones. 1.5 was chosen to be the lower limit of detecting peaks near  $\pi/2$ ; however, this rounding could be a source of error if  $\phi$  rises above 1.5 and descends naturally, which would then be misread as a branch occurrence. This can happen in MTM where the C-parameters are frequency dependant. Once the sign branches are compensated for, the wave propagation must be recalculated with the proper sign branches in order to move on to the log branches.

The log branches occur when  $\phi$  reaches  $\pi$ . Similar to solving for the sign branches, these peaks may be detected using the `findpeaks()` function of MATLAB. However, if the C-parameters are not constant over frequency, then it's possible to get a negative log branch. The code shown in Listing 5.2 properly compensates for log branches. `m2` was initialized as an array of zeros, and `cumsum()` will progressively add the log branches across the array. `val` is used to determine whether to increase or decrease the branch value. Looking at a peak, if  $\phi^{-pks} > 0$ , then the log branch is positive because  $\phi$  is increasing and the next value of  $\phi$  needs to be added  $2\pi$  to maintain continuity. However, if  $\phi^{-pks} < 0$ , then the branch is negative because  $\phi$  is decreasing and the current value of  $\phi$  needs to be subtracted  $2\pi$ . There is still a potential source of error with this code; if  $\phi$  rises and falls between 3 and  $\pi$ , a similar error to the one previously described, this code will misread the event as a log branch.

Listing 5.3. MATLAB code for sign branch of (2.40) in ENG

```
1  zr = zr.*(1-2*( (X>1) & (imag(s11)>0) ));
```

### 5.3. ENG and MNG Adjustments

For ENG systems,  $Z_r$  has a similar instability as  $e^{\gamma^d}$  did for DPS. Consequently, it has a similar solution. Because of an imaginary component floating near zero in the root of Eqn. (2.40),  $Z_r$  can be unstable if it is expected to be primarily imaginary. The same two solutions can be applied here. Either multiply the inside of the root by  $-1$  and the outside by  $j$  or, since it has been found that the imaginary component is negligible in comparison to the real component, removing the imaginary component entirely attributing it to computer error. The theoretical validity of this action may be disputed, but it will be performed for the remainder of this paper as it simplifies calculations for all quadrants.

Equation (2.40) has a  $\pm$ , which is usually decided by Eqn. (4.1a); however in this quadrant  $Real[Z_r] = 0$ , therefore the assumption is not helpful in determining the proper sign of  $Z_r$ . Since  $X > 1$  for only ENG and MNG and  $Imag[S_{11}] > 0$  for ENG, which was discovered in testing values, these together can be used as an assumption to determine that the current sample is ENG. According to TABLE 5.2, for ENG  $Sign[Z_r] = -j$ , therefore the  $\pm$  of Eqn. (2.40) should be chosen to be negative for ENG. This concept is practiced in Listing 5.3 and can be run as a final step of the code.

Though, in ENG  $X$  can be quite large, depending on the situation. In the simulations used for this paper, when  $f > 10$  [GHz],  $X \gg 10^7$  for some simulations. If  $X^2 > 10^{16}$ , this is a problem for Eqn. (4.2) as MATLAB, by default uses double floating point precision, which only holds about 16 digits, as according to [18]. Since  $X^2 \gg 1$ ,  $\sqrt{X^2 - 1} = X$  and  $e^{\gamma^d} = 0$ . This is incorrect and causes  $n = \infty$ . (Note that there is not a gradual convergence to these values, but rather a sudden occurrence; thus the statement " $e^{\gamma^d} \rightarrow 0$ " is not used.) To increase precision beyond double floating-point in MATLAB,  $X$  was stored as a *sym* from the Symbolic Math Toolbox. This allowed Eqn. (4.2) to be processed with 100 digits of precision and eliminated the issue of  $X$  being too large. This concept is practiced in Listing 5.4. Note that *pro* is immediately stored as a double

Listing 5.4. MATLAB code for symbolic math calculation of (4.2)

```

1  if any(X > 1e7)
2  X = sym((1 + s21.^2 - s11.^2)./s21/2);
3  pro = double(...
4  real(X) + m1.*sqrt(real(X).^2 - 1));
5  X = double(X);
6  else
7  pro = ...
8  real(X) + m1.*sqrt(real(X).^2 - 1);
9  end

```

Listing 5.5. MATLAB code for  $m_1$  selection in ENG and MNG

```

1  m1 = (m1 + 1).*(real(X) < 1) - 1;

```

floating-point value, so as to keep that the default class. Also note the if statement to catch if  $X$  is ever large enough to justify using the *sym* class.

Finally, for ENG it is found that the proper sign branch is  $m_1 = -1$ . This can be implemented with the code in Listing 5.5, which again uses  $X > 1$  as the indication of ENG. This code should be used at the end of Listing 5.1.

All adjustments mentioned in this section are also needed for MNG. The code listings shown will also work in discerning ENG from MNG.

#### 5.4. DNG Adjustments

The adjustments made for DPS are also needed for this quadrant, with one addition. The methods to select  $m_1$  and  $m_2$  are mostly correct, but will be negative of what it should be in DNG. When it comes to deciding if a sample is DPS or DNG, it is rather difficult to recognize as most of the values from the equations in section 2.5.3 will be the same for both quadrants. However, the wave propagation and S-parameters show a slight distinction.

In addition to the criteria that  $X < 1$ , which determines that the sample is either DPS or DNG, the sign of phase of the wave propagation can be used to distinguish the two quadrants. For DPS,  $\sqrt{\mu\epsilon} > 0 \Rightarrow \phi > 0$ , where the phase  $\phi = \beta d$  and  $\beta$  is the phase constant; and for DNG,  $\sqrt{\mu\epsilon} < 0 \Rightarrow \phi < 0$ . Thus the sign of  $\phi$  is the distinguishing factor between DPS and DNG. However, as the equations are currently written,  $\phi$  is by default positive, unless the signs of  $m_1$  and  $m_2$  are changed; thus  $\phi$  suffers the same need for correction as  $m_1$  and  $m_2$ . However, interestingly it has been found that  $\phi \approx -\angle S_{21}$ , after  $m_2$  branch corrections.

Listing 5.6. MATLAB code for  $m_1$  and  $m_2$  sign correction in DNG

```

1  as21 = angle(s21);
2  das21 = [0; diff(as21)];
3  [~, pks] = findpeaks(max(abs(das21), 6));
4  val = sign(das21(pks));
5  m3 = m2*0;
6  m3(pks) = val;
7  m3 = cumsum(m3);
8  isDPS = 1-2*(as21 - 2*pi*m3 > 0).*(X < 1);
9  m1 = m1.*isDPS;
10 m2 = m2.*isDPS;

```

Since  $\angle S_{21}$  modulates to be between  $\pm\pi$ , it is discontinuous unless added  $-2\pi m_2$ . This is the same  $m_2$  from Eqn. (4.3). However,  $m_2$  may have the wrong sign, and the branches may be off by a single frequency sample. To fix this, a third branch must be analyzed. This branch is the same type as  $m_2$ , thus it may have the same solution. In order to ensure accuracy, the first derivative was analyzed instead. The code in Listing 5.6 creates  $m_3$  and uses it on  $\angle S_{21}$  to determine if a sample is DNG or DPS. `diff(...)` is providing the first derivative of  $\angle S_{21}$ , however it returns an array one element less than its input, thus 0 is concatenated as the first element. `findpeaks(...)` works just as it did for Listing 5.2, but the input is a little different this time. Whenever there is a branch, `das21` will spike to  $\pm 2\pi$ , as the uncompensated  $\angle S_{21}$  is jumping either  $\pi \rightarrow -\pi$  or  $-\pi \rightarrow \pi$ ; thus checking for spikes beyond  $\pm 6$  should indicate a branch. Since `findpeaks(...)` only looks for positive peaks, the absolute value was used. Since this results in a loss of information, knowing whether a spike is positive or negative, its sign is stored in the `val`.  $m_3$  is then initialized as zeroes and computed with these values just as  $m_2$  was. To check if a sample is DPS,  $X$  must not be greater than 1 and the branch corrected  $\angle S_{21}$  must not be positive. If both these tests fail, then the sample is DNG and  $m_1$  and  $m_2$  are flipped at those samples only.

Thus, with these adaptations of MATLAB code combined with the phase tracking method of the previous chapter and further illustrated in this chapter, the C-parameters may be derived from the S-parameters sampled over a range of frequencies for any dielectric MTM.

## 6. RESULTS

Here are the results of a series of tests featuring both HFSS and MATLAB simulations and highlighting the phase tracking method's strengths and weaknesses.

The results of this developed phase tracking method are shown in Fig. 6.1 and 6.2. These results use the 20 HFSS simulations from Table 5.1 and Fig. 5.1.

One of the advantages of using vector calculations is that MATLAB is optimized for array and matrix calculations, thus it is more efficient than using **for** loops and nested **if** statements. Performing results on a Intel I3-4170 (3.70GHz, Dual Core) with 12 GB of RAM and Windows 10 (ver. 1803) are shown in Table 6.1.

As for accuracy, the phase tracking method consistently stays below 3.2 [%] average error. DPS and DNG clearly show the branch compensation may be off by a sample, causing spikes in the results. Simulations which have ENG or MNG use the symbolic toolbox for increased accuracy, but also seem to have the highest error. As  $n$  increased, particularly to the range where  $X > 10^{10}$ , as shown in Fig. 6.3. Here is the simulation with the greatest error in  $n$ , with growing error from -1 [%] at 11.3 [GHz] to -14.6 [%] at 20 [GHz], and averaging 3.1 [%].

The MATLAB simulations read less error than that of the HFSS simulations. This is likely due to two major causes: the first being that the math to produce the S-parameters is almost the same math as to produce the C-parameters in MATLAB, whereas the algorithms of HFSS are much more complicated; and the second being that there may be information loss in the data

Table 6.1. Average performance times and max error for various tests on a Intel I3-4170 (3.70GHz, Dual Core) with 12 GB of RAM and Windows 10 (ver. 1803). Note that the only tests that will use **sym()** are tests detecting ENG or MNG ( $X > 1$ ). Error is calculated as the mean of absolute value of percent difference per simulation with the max error per simulation set shown. \**Mean over whole set.*

Tests	Frequencies	$X > 1$	Platform	Time (mean)	Error (max)
1	381	No	HFSS	2.6 [ms]	1.7 [%]
1	381	Yes	HFSS	690 [ms]	3.2 [%]
20	381	50 [%]	HFSS	4.1 [s]	*0.7 [%]
1	20,000	no	MATLAB	800 [ms]	$8.2 \times 10^{-13}$ [%]
1	20,000	Yes	MATLAB	3.8 [s]	$4.5 \times 10^{-4}$ [%]
4	20,000	50 [%]	MATLAB	6.8 [s]	* $2.3 \times 10^{-4}$ [%]



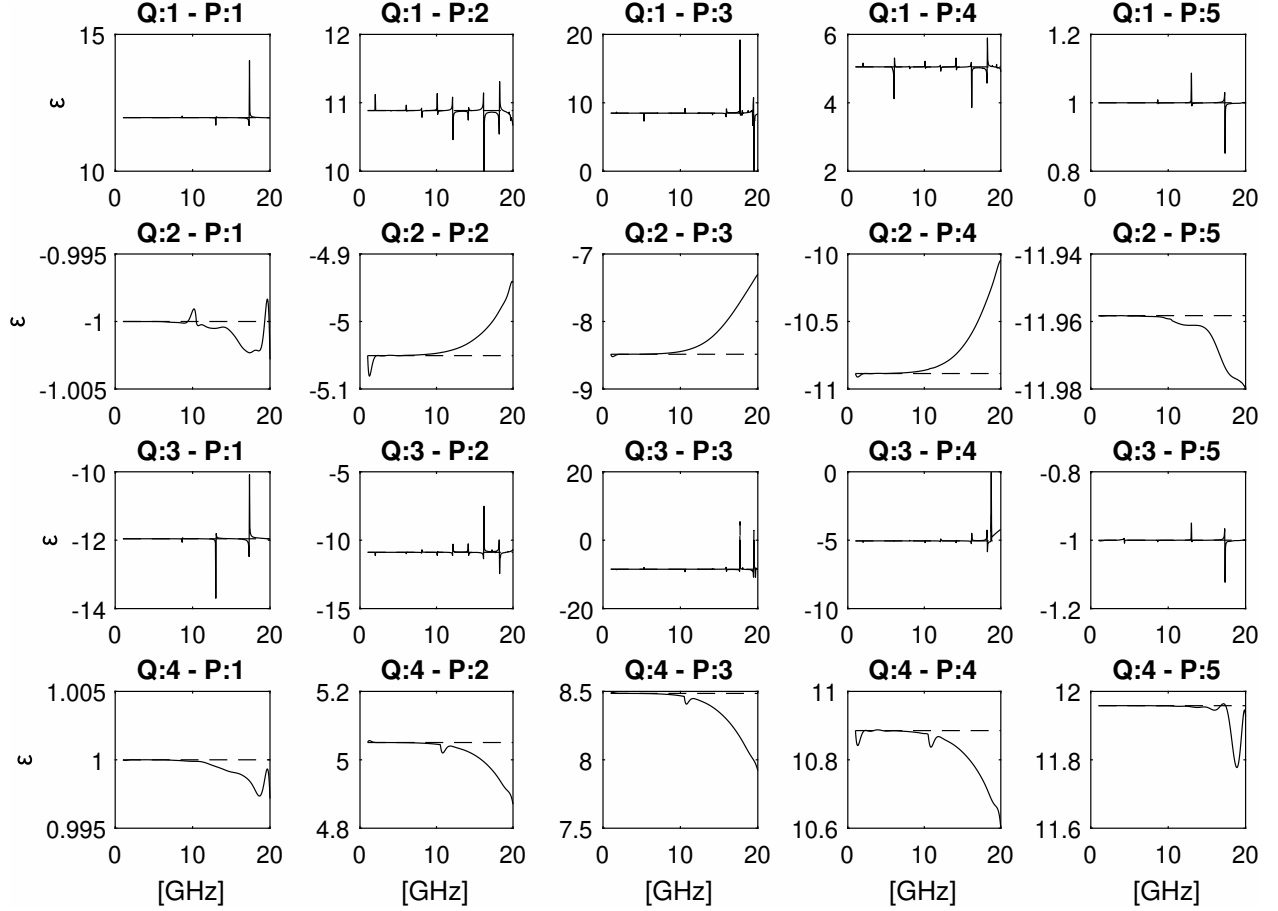


Figure 6.1. Results of deriving  $\varepsilon$  from HFSS simulations based on data from Table 5.1 and Fig. 5.1 using automated phase tracking for branch compensation. The solid line (—) is the phase tracking results and dashed line (- -) is the expected value. Each title denotes the quadrant (Q) and point (P) of MTM based on Fig. 5.1.

transfer between HFSS and MATLAB for analysis. The latter, being that HFSS exports 6 digits of precision, whereas MATLAB by default stores approximately 15 digits of precision. The former, being that HFSS is designed to account for impurities and many other possibilities, thus may be more unstable due to the added theory in the algorithms. However, which is to be considered the more accurate platform? While HFSS is likely to have little errors due to the presence of multiple algorithms, and possible user error as it is a very complex software, HFSS is less likely to have major flaws in it's results. Whereas the algorithms in MATLAB are quite controlled and simple, thus reducing the possibility of minor errors, but is also unsupported by teams and communities, thus more likely to experience major errors. This is why it is necessary to not only test with both, but

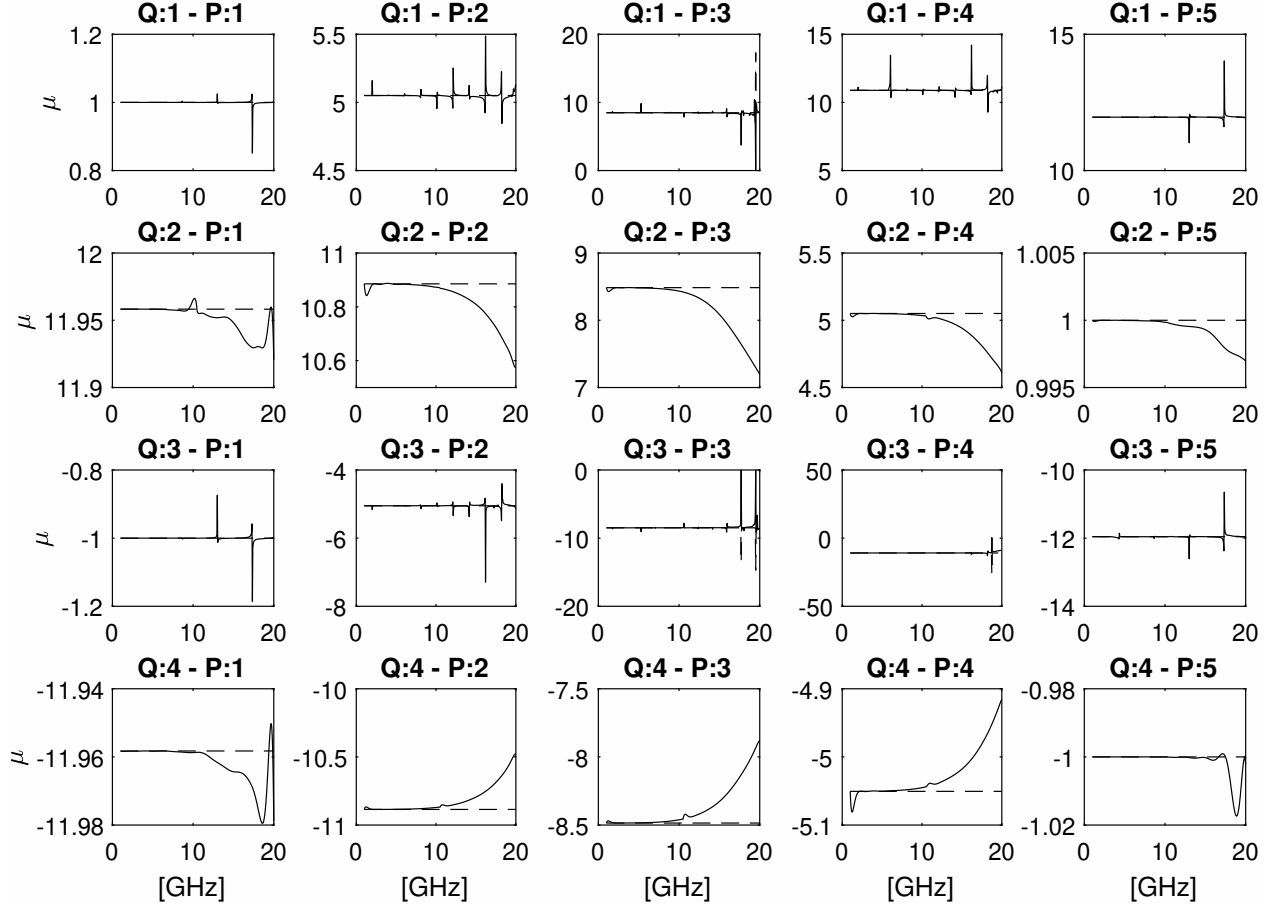


Figure 6.2. Results of deriving  $\mu$  from HFSS simulations based on data from Table 5.1 and Fig. 5.1 using automated phase tracking for branch compensation. The solid line (—) is the phase tracking results and dashed line (- - -) is the expected value. Each title denotes the quadrant (Q) and point (P) of MTM based on Fig. 5.1.

also to compare the two in order to verify the preliminary theory that building the phase tracking method is founded on.

Comparing MATLAB's theory to HFSS's simulation in producing the S-parameters from defined C-parameters, the results are very similar. The average difference between  $S_{11}(\text{HFSS})$  and  $S_{11}(\text{MATLAB})$  is 1.2 [%], with one exception. Because of its simplicity, MATLAB can return exact numbers for certain situations. For point 3 of all quadrants  $\varepsilon = \mu$ , thus  $Z_r = 1 \Rightarrow Z = Z_0$  and there will be no reflection ( $S_{11} = 0$ ). While MATLAB returns  $S_{11} = 0$ , HFSS returns  $S_{11} = 0^+$ .

This method has also been tested against non-constant C-parameters. Figures 6.4 and 6.5 show the results of phase tracking with a sinusoidal value of  $\varepsilon$  and constant  $\mu$ . This works with varying  $\varepsilon$  and/or  $\mu$ . However, this method is prone to misjudging branches if there is too much

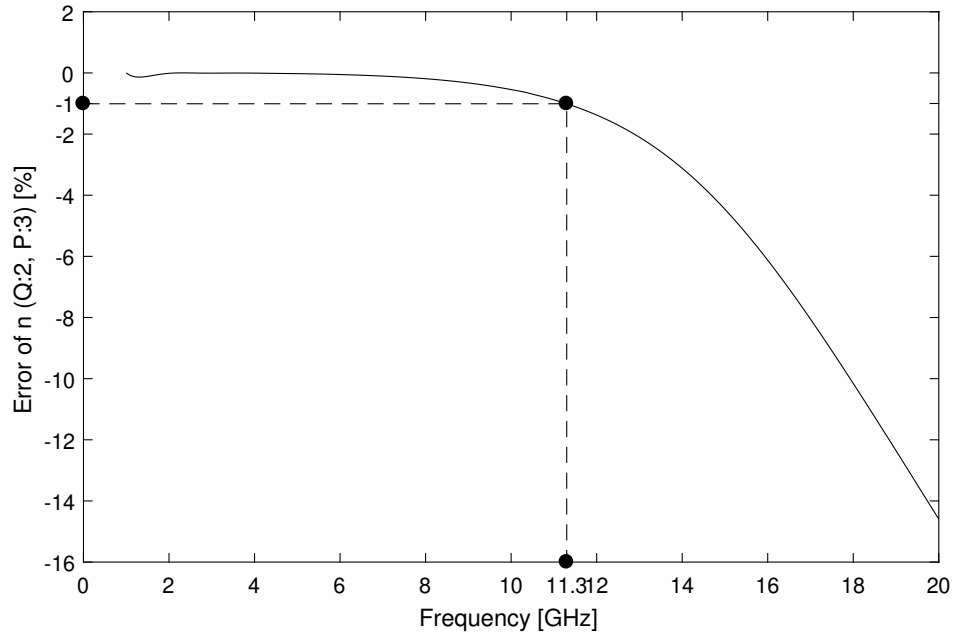


Figure 6.3. Error of Index of Refraction in ENG at point 3 of HFSS simulation. Error is likely due to the sensitivity of  $X$  increasing with frequency.

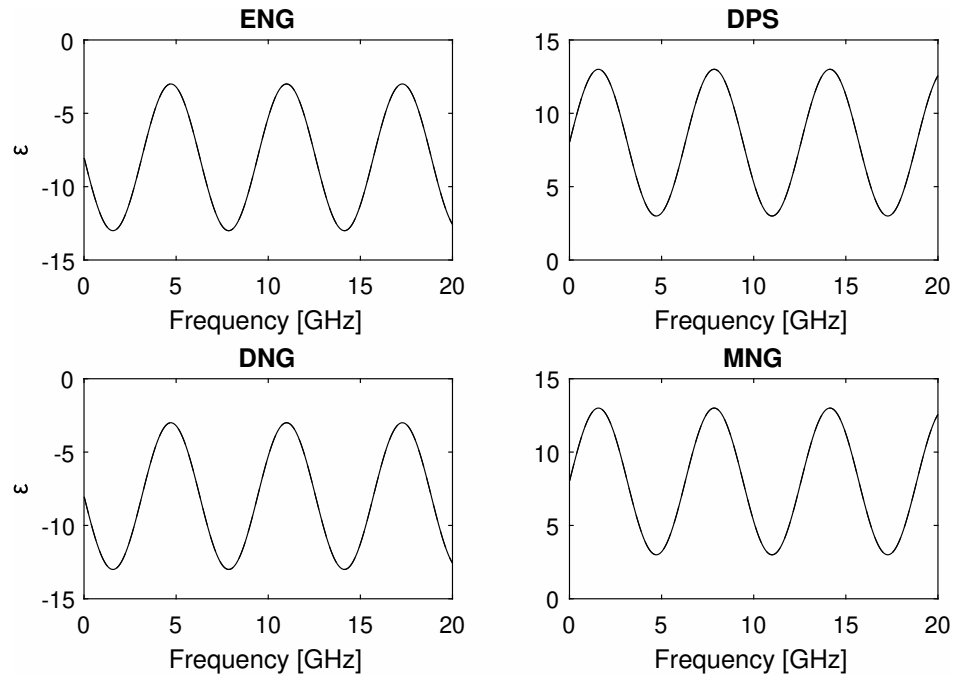


Figure 6.4. Results of deriving  $\varepsilon$  with phase tracking method using S-parameters from MATLAB simulation given  $\varepsilon = 8 + 5\sin(f/1e9)$  and  $\mu = 3$ .

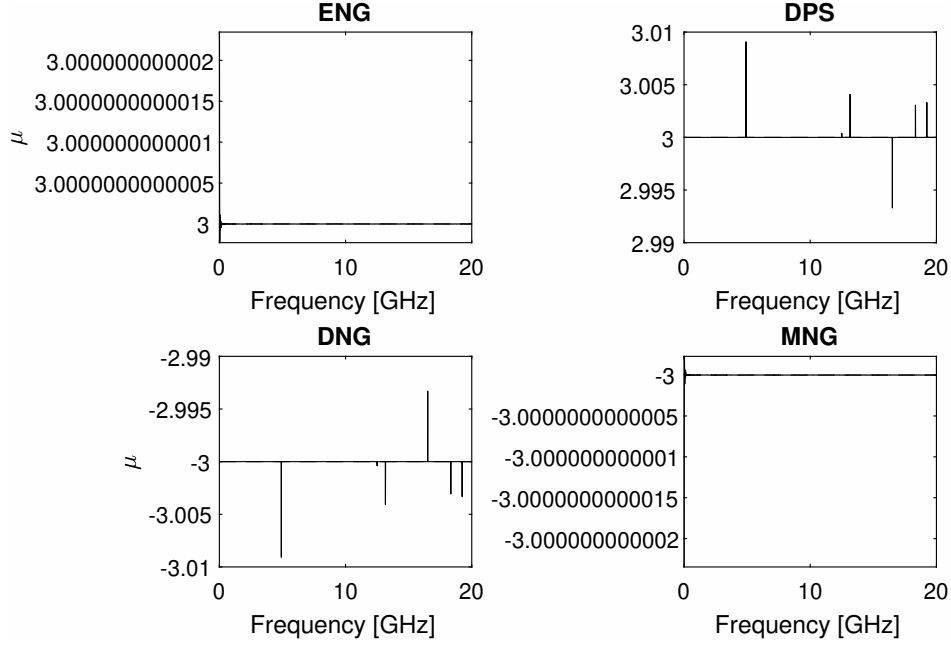


Figure 6.5. Results of deriving  $\mu$  with phase tracking method using S-parameters from MATLAB simulation given  $\varepsilon = 8 + 5\sin(f/1e9)$  and  $\mu = 3$ .

variation. This is likely due to the code in Listings 5.1 and 5.2 finding peaks that aren't actually jump cuts or branches. Figure 6.6 shows an example of a MATLAB simulation that had too much variance and produced erroneous results.

This method also works with  $\varepsilon$  crossing from positive to negative or visa versa in a single simulation, as shown in Fig. 6.7 However it does not currently handle a second zero crossing well, as shown in Fig. 6.8.

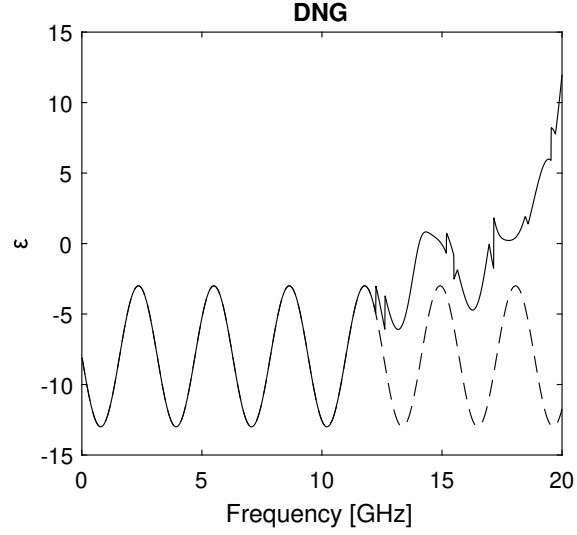


Figure 6.6. Results of deriving  $\varepsilon$  with phase tracking method using S-parameters from MATLAB simulation given  $\varepsilon = 8 + 5\sin(f/1e9)$  and  $\mu = 5 + 3\cos(f/1e9)$ . Code produces bad branch choices after 12.24 [GHz].

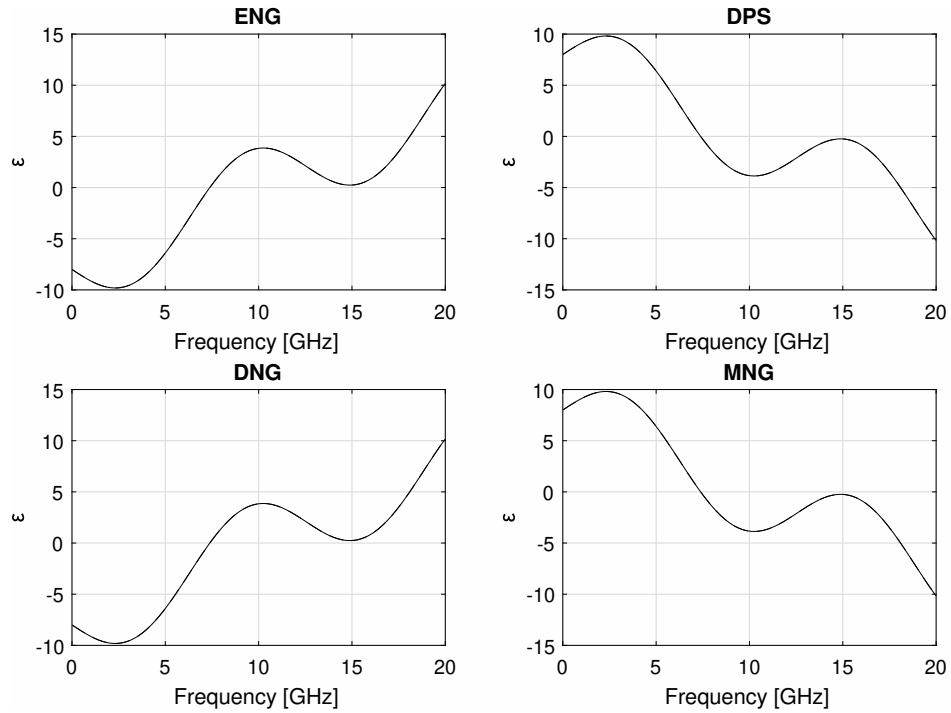


Figure 6.7. Results of deriving  $\varepsilon$  with phase tracking method using S-parameters from MATLAB simulation given  $\varepsilon = 8(1 - f/1e10) + 4\sin(f/2e9)$  and  $\mu = 2$ . Note that  $\varepsilon$  is crossing  $\varepsilon = 0$  once, thus changing the metamaterial quadrant mid simulation.

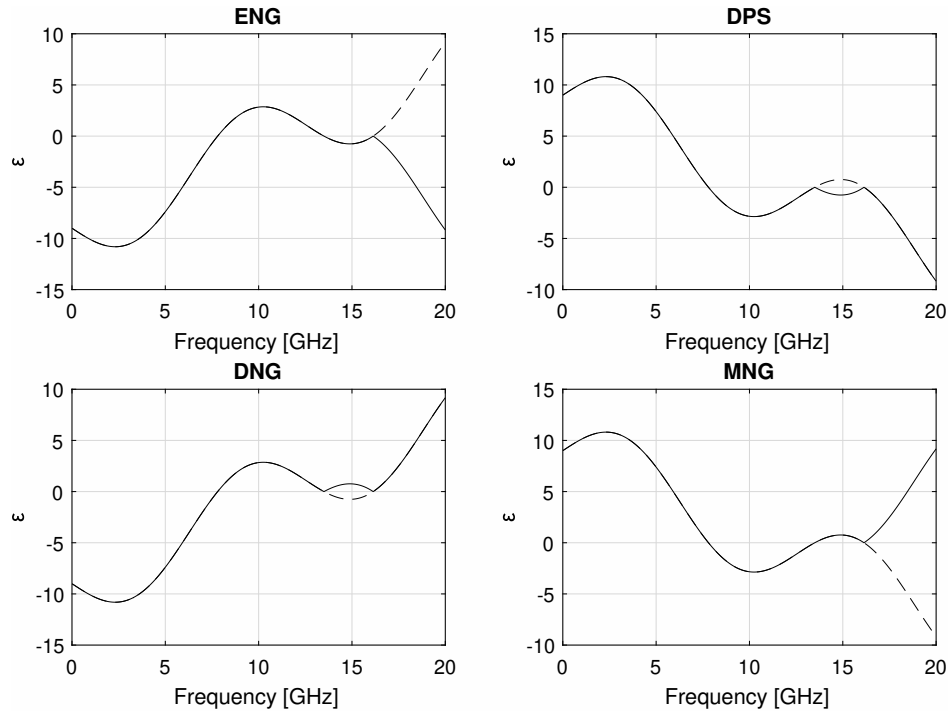


Figure 6.8. Results of deriving  $\epsilon$  with phase tracking method using S-parameters from MATLAB simulation given  $\epsilon = 8(1 - f/1e10) + 1 + 4\sin(f/2e9)$  and  $\mu = 2$ . Note that  $\epsilon$  is crossing  $\epsilon = 0$  3 times, thus changing the metamaterial quadrant mid simulation but showing errors.

## 7. CONCLUSION

The goal was to solve the C-parameters from the S-parameters of a dielectric metamaterial, including a thorough analysis in branches and compensating them. This thesis started with the mathematical derivation of the C-parameters from the S-parameters. Chapter 2 provided a detailed derivation of the C-parameters in terms of the S-parameters; chapter 3 looked at detecting branches; chapter 4 introduced the phase tracking method; chapter 5 expanded phase tracking for all quadrants of metamaterial and looked at MATLAB code for this method; finally chapter 6 provided results confirming the accuracy and potential problems of the introduced method. With this method, engineers may analyze metamaterial systems like the dielectric slab, or expand the theory to account for differently designed systems. The greatest achievement of this thesis is definitely the theoretical analysis and compensation of branches in this system, thus it is my hope that anyone may benefit from this research for their applications or develop it further for greater accuracy and applicability to various systems.

### 7.1. Future Work

One of the assumptions of this thesis is that the system is considered lossless, which is not accurate to most, if any, systems in the natural world. Though this thesis focuses on branch management, the theory of phase tracking could be expanded to account for lossy systems.

Another assumption is that the system is homogeneous. Most metamaterials made today are structures which are not homogeneous. This phase tracking method could be expanded to account for non-homogeneous systems; however, on a macroscopic scale there may be no difference in the theory.

The theory from chapter 4 could be foundational to deciding if the branches have yet occurred for an unknown system based exclusively on the results from a single frequency test. If a simple test could be derived, it could save time in determining the C-parameters at any individual frequency below that of the first branch.

It is possible to reduce the chance of error in branch decisions by analyzing the first or second derivatives of  $\phi$  instead of  $\phi$  itself, as done in Listing 5.6.

## REFERENCES

- [1] J. R. Aguilar, M. Beadle, P. T. Thompson, and M. W. Shelley, “The microwave and rf characteristics of fr4 substrates,” in *IEE Colloquium on Low Cost Antenna Technology (Ref. No. 1998/206)*, Feb 1998, pp. 2/1–2/6.
- [2] J. B. Pendry, A. J. Holden, D. J. Robbins, W. Stewart *et al.*, “Magnetism from conductors and enhanced nonlinear phenomena,” *IEEE transactions on microwave theory and techniques*, vol. 47, no. 11, pp. 2075–2084, 1999.
- [3] J. Cleveland, B. D. Braaten, M. Allen, J. Allen, and B. Wenner, “On using micron-sized silver coated particles to control the electromagnetic response of a metamaterial with complementary split ring resonators and wires in a host dielectric,” *2018 IEEE Research and Applications of Photonics In Defense Conference (RAPID)*, 2018.
- [4] J. Cleveland, J. Lewis, D. Mitra, B. D. Braaten, J. Allen, and M. Allen, “On the phase shift of a microstrip transmission line loaded with magneto-responsive conducting micro-particles,” *IEEE International Symposium on Antennas and Propagation*, Jul 2020.
- [5] J. Cleveland, D. Mitra, J. Lewis, B. D. Braaten, J. Allen, and M. Allen, “On changing the impedance of a reactive surface using magneto-static responsive particles,” *2019 IEEE International Symposium on Antennas and Propagation and USNC-URSI Radio Science Meeting*, pp. 305–306, 2019.
- [6] —, “On the placement of particle containing cylindrical cavities in a grounded dielectric substrate to change the impedance of a printed reactive surface,” *2019 IEEE International Symposium on Antennas and Propagation and USNC-URSI Radio Science Meeting*, pp. 1901–1902, 2019.
- [7] E. J. Rothwell, J. L. Frasch, S. M. Ellison, P. Chahal, and R. O. Ouedraogo, “Analysis of the nicolson-ross-weir method for characterizing the electromagnetic properties of engineered materials,” *Progress In Electromagnetics Research*, vol. 157, pp. 31–47, 2016.



- [8] X. Chen, T. M. Grzegorzczuk, B.-I. Wu, J. Pacheco, and J. A. Kong, “Robust method to retrieve the constitutive effective parameters of metamaterials,” *Phys. Rev. E*, vol. 70, p. 016608, Jul 2004.
- [9] D. Hyun Lee and W. Sang Park, “Extraction of effective permittivity and permeability of periodic metamaterial cells,” *Microwave and Optical Technology Letters*, vol. 51, no. 8, pp. 1824–1830, 2009.
- [10] P. Markoš and C. M. Soukoulis, “Transmission properties and effective electromagnetic parameters of double negative metamaterials,” *Opt. Express*, vol. 11, no. 7, pp. 649–661, Apr 2003.
- [11] N. D. Orloff, N. Popovic, J. A. Drisko, A. Stelson, C. A. E. Little, J. C. Booth, J. Mateu, and C. J. Long, “How to extract distributed circuit parameters from the scattering parameters of a transmission line,” in *2017 90th ARFTG Microwave Measurement Symposium (ARFTG)*, 2017.
- [12] L. Si, W. Zhu, and X. Lv, “Determination of the effective constitutive parameters of active transmission line metamaterials,” in *2012 International Workshop on Metamaterials (Meta)*, Oct 2012.
- [13] D. R. Smith, W. J. Padilla, D. C. Vier, S. C. Nemat-Nasser, and S. Schultz, “Composite medium with simultaneously negative permeability and permittivity,” *Phys. Rev. Lett.*, vol. 84, pp. 4184–4187, May 2000.
- [14] D. R. Smith, S. Schultz, P. Markoš, and C. M. Soukoulis, “Determination of effective permittivity and permeability of metamaterials from reflection and transmission coefficients,” *Phys. Rev. B*, vol. 65, Apr 2002.
- [15] C. A. Balanis, *Advanced Engineering Electromagnetics*, 2nd ed. John Wiley & Sons, Inc., 2012.
- [16] J. Lewis, D. Mitra, J. Cleveland, B. D. Braaten, J. Allen, and M. Allen, “Theoretical explanation and prediction of branches in permittivity from s-parameter values,” *IEEE International Symposium on Antennas and Propagation*, Jul 2020.

- [17] —, “Theoretical explanation and prediction of branches in permittivity from s-parameter values,” *IEEE International Symposium on Antennas and Propagation*, Jul 2020.
- [18] IEEE, “Ieee standard for floating-point arithmetic,” *IEEE Std 754-2019 (Revision of IEEE 754-2008)*, pp. 1–84, 2019.

## APPENDIX

### A.1. SParam.m

```
1  %SParam.m
2  %[ s11, s21 ] = SParam( e, u, f, d )
3  % This code is to derive the Scattering Parameters from the Constitutive
4  % Parametres. Put in permittivity(e), permeability(u), frequency(f) and DEM
5  % thickness(d) and get reflection(s11) and transmission(s21). Use relative
6  % values for e and u. S-parameters will be complex values in non-dB form.
7  %
8  % Inputs:
9  %   e    Permittivity
10 %   u    Permeability
11 %   f    Frequency
12 %   d    Thickness
13 % Return:
14 %   s11  Reflection
15 %   s21  Transmission
16
17 function [ s11, s21 ] = SParam( e, u, f, d )
18     if nargin < 4
19         d = 0.001;
20         if nargin < 3
21             error( 'Not enough arguments' );
22         end
23     end
24
25     w = 2*pi*f;
26     c = 299792458;
27
28     g12 = (1-sqrt(u)./sqrt(e))./(1+sqrt(u)./sqrt(e));
29     phi = exp(-1j*w*d.*sqrt(e).*sqrt(u)/c);
30
31     s11 = -(g12.*(1-phi.^2))./(1-(g12.*phi).^2);
```

```
32      s21 = (phi.*(1-g12.^2))./(1-(g12.*phi).^2);  
33  
34  end
```

## A.2. CParam.m

```
1  %CParam.m
2  % This code is to derive the Constitutive Parameters from the Scattering
3  % Parametres and some other data.
4  %
5  % Inputs:
6  %   f      Frequency
7  %   s11     Reflection
8  %   s21     Transmission
9  %   d      Thickness
10 %   m1     Sign branch
11 %   m2     Log branch
12 % Return:
13 %   e      Permittivity
14 %   u      Permeability
15 %   n      Index of refraction
16 %   zr     Relative Intrinsic Impedance
17 %   egd    Wave propagation  $\langle e^{(j \gamma d)} \rangle$ 
18 %   X      Variable used in calculating egd  $\langle egd = X \pm \sqrt{X^2 - 1} \rangle$ 
19
20 function [zr, n, pro, X, Yn, Yd] = CParam(f, s11, s21, d, m1, m2)
21     % Define constant and w
22     c = 299792458;
23     w = 2*pi*f;
24
25     % Solve Stuff
26     X = (1 + s21.^2 - s11.^2)./s21/2;
27     % If there will be loss of information due to the largness of X^2
28     if any(X > 1e7)
29         X = sym((1 + s21.^2 - s11.^2)./s21/2); % Convert to symbol
30         % Use Symbolic Math
31         pro = double(real(X) + m1.*sqrt(real(X).^2 - 1));
32         X = double(X); % Convert back to double
33     else
34         pro = real(X) + m1.*sqrt(real(X).^2 - 1);
35     end
```

```

36     n = (-1j*log(pro) + 2*pi*m2)*c./w/d;
37
38     % Two different calculations for if Zr is primarily real or imaginary
39     Yn = s21.^2 - (1 + s11).^2;
40     Yd = (s21.^2 - (1 - s11).^2);
41     zr = sqrt(real(Yn./Yd));
42 end

```

### A.3. phase\_tracking.m

```
1  %phase_tracking.m
2  % Written by Jacob Lewis May 2020.
3  % The purpose of this program is to take the S-parameters accross a
4  % spectrum of frequencies to calculate the C-parameters of a substrate ,
5  % compensating for branches and accounting for every quadrant of
6  % metamaterial. Though all values returned are complex, an assumption of
7  % the substrate is that it is lossless and thus the values may not be
8  % accurate if they indicate a level of loss or gain (such as imaginary
9  % permittivity , permeability or negative impedance). All values returned
10 % will be arrays of type "complex double". All arrays given and returned
11 % should be the same size (except for d which is scalar). The S-parameters
12 % should be complex doubles and f and d should be real.
13 %
14 % Given:
15 %   f      Frequency
16 %   s11    S11
17 %   s21    S21
18 %   d      Substrate thickness (scalar, real)          *OPTIONAL, Default: 0.01 *
19 % Return:
20 %   e      Permittivity
21 %   u      Permeability
22 %   n      Index of refraction
23 %   z      Impedance
24 %   pro    Wave propagation  $\langle e^{(j \gamma d)} \rangle$ 
25 %   X      Used to compute  $\epsilon d \langle \epsilon d = X \pm \sqrt{X^2 - 1} \rangle$ 
26 %   m1     Sign branch
27 %   m2     Log branch
28
29 function [e, u, zr, n, pro, X, Yn, Yd, m1, m2] = phase_tracking(f, s11, s21, d)
30
31     if nargin < 4
32         d = 0.01;    % d = 1 [cm]
33     end
34
35     % Start with these intial conditions
```

```

36     m1 = ones(size(f)); % Sign branch is positive
37     m2 = m1*0; % Log branch is 0
38
39     % Calculate C-parameters
40     [~, ~, pro, X, ~] = CParam(f, s11, s21, d, m1, m2);
41
42     % Find sign branches
43     phi = angle(pro); % Angle of wave propagation
44     phin = abs(phi-pi/2); % Normalize to pi/2 and take abs
45     % Local peaks above 1.5 of phin are the sign branches
46     [~, pks] = findpeaks(max(phin,1.5)); % Signal Processing Toolbox
47     m1(pks) = -1; % Assign the peaks to -1 as inflection points
48     m1 = cumprod(m1); % Carry changes throughout
49     m1 = (m1 + 1).*(real(X) < 1) - 1; % m1 = -1 for ENG/MNG
50
51     % Recalculate Sign Branch Corrected C-parameters
52     [~, ~, pro, ~, ~] = CParam(f, s11, s21, d, m1, m2);
53
54     % Find log branches
55     phi = angle(pro); % Angle of wave propagation
56     % Local peaks above 3 of phi are the log branches
57     [~, pks] = findpeaks(max(phi,3));
58     val = phi(pks - 1) > 0; % val is for determining the sign of the branch
59     % +- branch count ['just after', 'at'] branch location
60     m2(pks + val) = 2*val - 1;
61     m2 = cumsum(m2); % Carry changes throughout
62
63     % Check if DNG
64     as21 = angle(s21); % Angle of S21
65     das21 = [0; diff(as21)]; % Diff of angle of S21
66     [~, pks] = findpeaks(max(abs(das21),6));
67     val = sign(das21(pks));
68     m3 = m2*0; m3(pks) = val; m3 = cumsum(m3);
69     isDPS = 1-2*(as21 - 2*pi*m3 > 0).*(X < 1);
70     m1 = m1.*isDPS; m2 = m2.*isDPS;
71

```



```

72      % Recalculate Log Branch (and DNG) Corrected C-parameters
73      [zr, n, pro, X, Yn, Yd] = CParam(f, s11, s21, d, m1, m2);
74
75      % Correct sign of zr for Q2
76      zr = zr.*(1-2*( (X>1) & (imag(s11) > 0) ));
77
78      u = n.*zr;
79      e = n./zr;
80
81  end

```